# Characterization of Fouling of Tertiary Membranes Treating Secondary Effluent of Domestic Wastewater

by

Sara Abu-Obaid

A thesis
presented to the University of Waterloo
in fulfillment of the
thesis requirement for the degree of
Master of Applied Science
in
Civil Engineering (Water)

Waterloo, Ontario, Canada, 2018

©Sara Abu-Obaid 2018

# AUTHOR'S DECLARATION

I hereby declare that I am the sole author of this thesis. This is a true copy of the thesis, including any required final revisions, as accepted by my examiners.

I understand that my thesis may be made electronically available to the public.

# Abstract

The use of membranes for tertiary treatment of wastewater has become more frequent over the years, especially with increasing interest in water reuse. Fouling prevents wider application of this technology as it creates operational challenges and increases costs. In tertiary applications, membrane feedwater can be variable in composition as this depends on the operating conditions of the implemented upstream biological treatment process. The tertiary membranes at the Keswick WPCP have demonstrated increased fouling in the spring season. Early spring marks the period that corresponds to low wastewater temperatures and elevated flows. This study sought to identify critical operating conditions leading to seasonal fluctuations in fouling of full-scale tertiary membranes. This was done through conducting a detailed historical review of membrane operational parameters for the year of 2016 and 2017. In addition, changes in potential foulants during high fouling periods were examined to obtain an improved understanding of the foulant characteristics. This was done through a sampling campaign that spanned multiple seasons of operation aiming to characterize feedwater quality during extreme operational conditions.

The analysis of historical data revealed a relationship between membrane fouling and water temperature and flow, which was more than could be explained by changes in water viscosity with temperature. However, it was observed that the membrane fouling behavior significantly differed between the two year-long observation periods, with a peak in fouling indexes during March and April for 2016, and inconsistent fluctuations in fouling indexes between January and May for 2017. The differing patterns suggested a complex dependence of fouling on the operating conditions. Therefore, it was concluded that fouling depends on water temperature and flow, however, it was not possible to delineate the contributions of the individual variables as they were found to be highly correlated.

The examination of feedwater characteristics data revealed that high membrane fouling rates correlated to an increase in biopolymer concentration of total DOC. The increase in biopolymer concentration was also correlated to a decrease in water temperature and increase in flow. However, no relationship was observed between TOC/DOC concentrations and temperature and flow. This could indicate that fouling of tertiary membranes due to seasonal variation in operational conditions is a result of alterations to the composition of organics in membrane feed, not the overall concentration

of TOC/DOC. The examination of field data also revealed an increase in CST values during high fouling events. The increase in CST values correlated to the decrease in water temperature and increase in flow. Elevated CST values, which indicate worsened dewaterability of sludge, also correlated to higher biopolymer concentrations. Therefore, it was concluded that seasonal variations may result in the increased release of EPS by microorganisms. This leads to higher membrane fouling and worsened dewaterability of upstream sludge.

The results of this study enhance the knowledge of fouling behaviour and foulant characteristics for tertiary membranes operating under stressed conditions. This knowledge will be of value when designing mitigation strategies to reduce the costs of these types of systems.

# Acknowledgements

I would like to start off by expressing my deepest gratitude to my supervisor Prof. Wayne Parker for his support, guidance, and immense knowledge. Your patience, motivation, and welcoming attitude is the reason my graduate experience at the University of Waterloo was of great value. I appreciate the endless hours you spent listening to my thoughts and theories regarding this project allowing me to grow on my own as a researcher, while helping me pave my academic path. In addition, I would like to express my warmest gratitude to my other supervisor Prof. Pierre Berube. Your guidance has enabled the expansion of the scope of this project, morphing it into the work that I proudly present today.

Furthermore, a special thanks to Jun Liu, Virgil Turtulli, Jefferson Wu and Jason Holmes from the Region of York for the incredible amount of help they offered, as well as providing me with access to the data and samples used for the completion of this project.

I would also like to acknowledge that LC-OCD samples were measured at the NSERC Industrial Research Chair in Water Treatment at the University of Waterloo, Ontario, Canada. Thank you to Lin Shen and Rachel Trouwer for operating the LC-OCD and to Dr. Sigrid Peldszus for managing it.

Finally, I would like to express my greatest appreciation for the love and support of my family and friends. From within that category fall my dear friends; Mulham Akhras and Mohannad Mostafa, their guidance with some aspects of this project is truly appreciated. Thank you all for everything.

# Table of Contents

# List of Figures

# List of Tables

## List of Acronyms

**BP:** Back-pulse

**$cBOD_5$:** Carbonaceous biological oxygen demand

**COD:** Chemical oxygen demand

**CST:** Capillary suction time

**DOC:** Dissolved organic carbon

**DON:** Dissolved organic nitrogen

**FI:** Fouling index

**F/M:** Food to microorganism ratio

**EPS:** Extracellular polymeric substances

**HP-SEC:** High performance size exclusion chromatography

**HRT:** Hydraulic retention time

**LC-OCD:** Liquid chromatography- Organic carbon detection

**LMW:** Low molecular weight

**MBR:** Membrane bioreactor

**MC:** Maintenance clean

**RC:** Recovery clean

**SMP:** Soluble microbial products

**SRT:** Solids residence time

**SUVA:** Specific ultraviolet absorbance

**TCP:** Temperature corrected permeability

**TC-TMP:** Temperature corrected transmembrane pressure

**TKN:** total Kjeldahl nitrogen

**TOC:** Total organic carbon

**TSS:** Total suspended solids

**UF:** Ultrafiltration

**$UV_{254}$ :** Absorbance of ultraviolet light at a wavelength of 254nm

**WPCP:** Water pollution control plant

# Chapter 1- Introduction

## 1.1 Background

Membrane technologies, which are traditionally used for drinking water treatment applications, have been increasingly employed in wastewater treatment in the past few decades (Citulski et al., 2009). In wastewater treatment membrane technologies are often implemented to improve effluent quality in response to more stringent regulations as well as a heightened interest in water reuse. Wastewater destined for reuse must meet high quality standards regarding suspended solids and pathogen concentrations, which can be met using membranes that act as physical barriers against particulate material and microorganisms (Arévalo et al., 2009). Membrane technologies are typically incorporated into the treatment train either as part of a membrane bioreactor (MBR) or for tertiary filtration downstream of secondary treatment (Kent et al. 2011). The advantages of membrane technologies include high efficiency and reliability, low space requirements, and an absence of by-product generation (ToràGrau et al., 2014). However, the widespread application of this technology is somewhat limited by fouling that can lead to a decline in membrane permeability and overall performance (Ma et al. 2013). Fouling of membranes leads to the need for backwashing and chemical cleaning, thereby increasing the cost of operation and shortening lifespans (Abdullah and Bérubé 2013). While capital costs of membrane projects have decreased dramatically over the last years due to the decrease in membrane module costs, fouling leads to elevated energy demand making it the main contributor to overall MBR operating costs (Drews, 2010).

Membrane materials, feedwater characteristics, operational conditions and biomass characteristics have been reported to influence the performance of membranes employed for wastewater applications (Meng et al., 2009; Sweity et al., 2011). In tertiary applications, membrane feedwater can be variable in composition as this depends on the efficiency of the upstream secondary treatment, which will be influenced by raw wastewater characteristics and the operating conditions of the implemented biological treatment (ToràGrau et al., 2014). Some of the operating conditions which can influence membrane fouling include solids residence time (SRT), hydraulic retention time (HRT), and temperature (Drews, 2010). Seasonal fluctuations in raw wastewater temperature and flow, which affects HRT, can influence bioreactor performance and consequently the foulant characteristics of membrane feed streams.

## 1.2 Problem Statement

The Keswick Water Pollution and Control Plant (WPCP) in the Region of York, Ontario, Canada, is an example of a plant employing tertiary ultrafiltration (UF) membranes to treat municipal wastewater. Substantial deterioration in the performance of the membranes, which are employed downstream of the activated sludge process has been consistently observed during the early spring period (March to May). Early spring marks the period that corresponds to low wastewater temperatures and elevated flows. Several studies of seasonal deterioration of membrane performance in MBRs due to low operating temperatures have been reported (Sun et al., 2014, Al-Halbouni et al., 2008., Rosenberger et al., 2006, van der Brink et al., 2011). There are however few reports of the effect of seasonal variations on the fouling of tertiary membranes. It can be anticipated that tertiary membranes, which are not as exposed to settleable components, will have different fouling mechanisms, and therefore, may be differently affected by operating conditions. Hence, there is an evident need for studies focused on factors affecting fouling of tertiary membranes.

A number of papers that addressed fouling of MBR membranes under cold water conditions have been published in the last 10 years. Some studies have suggested that membrane performance declines at low temperatures due to reduced recovery of flux after cleaning under such conditions (Martín-Pascual et al., 2015). Pore blocking (i.e. irreversible fouling) as a result of increased concentrations of supernatant organics has also been identified as a cause of increased fouling (Sun et al., 2014, van den Brink et al., 2011). It has been proposed that these organics may arise from either reduced hydrolysis of potential foulants from influent wastewater (Krzeminski et al., 2011) or increased release by biomass under low temperature conditions (Gao, 2013). The lack of consensus on the main fouling mechanisms under cold water conditions demonstrates the need for further investigation.

A number of studies have examined fouling of MBRs under cold water conditions. However, there are very few reports of the effect of elevated flows (especially seasonal variations that lead to dynamic fluctuations in flow) on membrane performance. These flows can directly influence HRT, which is a major operating parameter of bioreactors. Significant variations in raw wastewater inflow can also lead to fluctuations in the food to microorganism ratio (F/M) (Lyko et al. (2008)), which Kimura et al. (2005) have observed to be a major parameter affecting the nature of foulants.

Nonetheless, there is a clear lack of research on the effect of dynamic fluctuations of flow on membrane performance, especially for tertiary filtration applications.

## 1.3 Objectives

To address the knowledge gaps described in section 1.2, this research had two major goals;

1. To identify critical operating conditions (water temperature and feed flow) leading to the fouling of full-scale tertiary membranes.
2. To examine changes in potential foulants during high fouling events to obtain an improved understanding of the foulant characteristics.

The first goal was accomplished by conducting a detailed historical review of membrane operational parameters to achieve the following sub-goals:

1. Quantify fouling between consecutive back-pulses (BPs), maintenance cleans (MCs) and recovery cleans (RCs).
2. Quantify recovery of permeability during cleaning.

This work was completed for two representative trains (UF1, UF4) using raw data collected over the years of 2016 and 2017.

The second goal was accomplished by conducting a field study which involved an extended term sampling of the Keswick WPCP that spanned multiple seasons of operation. Membrane feedwater samples were collected and analyzed to accomplish the following sub-goals:

1. Track changes in conventional water characteristics including: pH, conductivity, temperature, turbidity, hardness, $UV_{254}$, TOC/DOC, $cBOD_5$/COD.
2. Track changes in various cation and anion concentrations including: $Ca^{+}$, $Mg^{+2}$, $K^{+}$, $Na^{+}$, $Br^{-}$, $Cl^{-}$, $Fl^{-}$, $SO_4^{-}$, and P.
3. Track changes in nitrogen species concentrations including: ammonia and $NH_4$, nitrate, nitrite, TKN and DON.
4. Measure concentrations of organic sub-fractions that are suspected membrane foulants including: biopolymers, humics, building blocks, low molecular weight acids (LMWa), and low molecular weight neutrals (LMWn) using liquid chromatography- organic carbon detection (LC-OCD).

Mixed liquor samples were also collected to characterize sludge dewaterability using the capillary suction time (CST) method.

This work was completed for 17-months starting in January of 2017 and ending in May 2018. This allowed for detailed characterization of fouling under two consecutive cold weather periods.

## 1.4 Thesis Structure

Chapter 2 consists of a literature review to provide an overview of the published material which is relevant to this work. Based on the literature review, research needs were identified and presented at the end of the chapter. Chapters 3 and 4 were each written as separate articles, and therefore they are intended to stand on their own, providing an introduction, materials and methods section, as well as discussion of the results and conclusions. Chapter 3 is a detailed historical review of membrane operational data to identify critical operating conditions leading to rapid deterioration of membrane permeability. The changes in foulant characteristics leading to higher fouling during critical operating conditions were investigated in the second portion of this study, and were reported in Chapter 4. Chapter 5 presents some of the major conclusions and implications of the results from Chapters 3 & 4, and offers recommendations for future work.

# Chapter 2- Literature Review

## 2.1 Observed membrane response to seasonal variations

There are many similarities between the two major applications of low-pressure membranes within wastewater treatment; tertiary membranes and MBRs. However, the membranes in MBRs interact with a range of potential foulants that span from truly soluble species to suspended solids, such as flocs (Rosenberger et al., 2006). It can be anticipated that in the case of tertiary membranes, which are not as exposed to settleable components, soluble and colloidal species will play a major role in membrane fouling. Hence, tertiary membranes will have different fouling mechanisms from MBRs, and therefore, may be differently affected by operating conditions. Few reports were found on studies specifically addressing the performance of tertiary membranes. The studies found are summarized in the section below.

### 2.1.1 Tertiary membranes studies

Three studies that focused on the performance of tertiary membranes were reviewed in detail. Kent et al., (2011) compared the permeate water quality of MBR and tertiary membrane pilot plants operating in parallel in a wastewater treatment plant. The activated sludge process ahead of the tertiary UF received the same feedwater as the MBR, and several water quality parameters (COD, TOC, color, SUVA, protein and polysaccharides) of the permeates were measured to compare the different treatment options. The results of the study displayed a decrease in average polysaccharides in the fall and winter in comparison to the spring. However, this was attributed to the change in method used for the measuring of polysaccharide concentrations between fall and winter, and the spring season. It was hypothesized that the increase in polysaccharide concentrations in the spring may have been due to either seasonal variation in the raw wastewater composition or temperatures. However, this study did not address membrane performance through fouling nor did it observe seasonal variations in performance.

Citulski et al., (2009) examined the role played by total suspended solids (TSS) on short-term fouling rates of a pilot-scale tertiary membrane. Membrane feedwater quality parameters such as pH, turbidity, TSS, $UVA_{254}$, TOC, and COD were collected across multiple seasons of operation. The study concluded that there were no seasonal trends in any of the water quality parameters measured, and that although water temperature fluctuated seasonally, membrane integrity was monitored

through the measure of biological indicators (total and fecal coliforms and somatic coliphages) showing that the membranes remained integral throughout the whole study. Therefore, although this paper addressed membrane performance through fouling, it did not track seasonal variations in performance.

Tora`-Grau et al., (2015) used a bench-scale UF setup to study membrane fouling behaviour using a simplified model wastewater containing only few compounds. The model water contained bovine serum albumin (BSA) as a protein and dextran as a carbohydrate. The water temperature was kept constant throughout the experiment (21$^{o}$C). This study did not address any seasonal variations in fouling as membrane feed characteristics were controlled as a part of the experiment.

### 2.1.2 Membrane bioreactors studies

In contrast to the lack of papers addressing the fouling of tertiary membranes in response to seasonal variations, multiple reports of the effect of seasonal variations on the fouling of MBRs were reviewed. Sun et al. (2014), Krezeminski et al., (2012), and Lyko et al., (2008) studied the effect of seasonal variations on fouling of MBRs treating domestic wastewater in full-scale plants. Krezeminski et al., (2012) focused on the effect of seasonal variations in temperature (6-23$^{o}$C) on raw domestic wastewater composition and MBR sludge filterability. This study concluded that seasonal fluctuations in membrane performance was a result of fluctuations in temperatures, with a deterioration in membrane performance during low-temperature periods. Sun et al., (2008) also observed an increase in filtration resistance with the decrease in water temperature. Lyko et al., (2008) not only observed higher membrane fouling during low-temperature periods. Deterioration of activated sludge dewaterability, and settleability were also observed under such conditions. This indicates that the operation of MBRs under cold water conditions can lead to changes in sludge characteristics.

Raw wastewater flows can also vary seasonally and it is hypothesized that this might impact upon the performance of systems that integrate biological and membrane processes. Lyko et al. (2008) reported that significant variations in the raw wastewater inflow resulted in changes in the F/M while Kimura et al. (2005) have observed that deviations in the F/M ratio of MBRs were a major contributor to

alterations to the nature of foulants. This indicates that seasonal fluctuations in flows can also lead to fluctuations in membrane fouling.

Several studies have examined the impact of seasonal variations in operating conditions on MBR membrane fouling at pilot-scale (Ma et al., 2013, Miyoshi et al., 2009, and Wang et al., (2010). Ma et al., (2013) and Wang et al., (2010) investigated the effect of temperature on membrane fouling. Both studies observed increased fouling under low-temperature operations. Wang et al., (2010) also reported changes in sludge characteristics due to seasonal variations in temperature (7-15 $^{o}$C) and observed a deterioration in the settling and dewaterability of mixed liquor under such conditions. The deterioration in settling and dewaterability can be an indicator of increased levels of extracellular polymeric substances (EPS) in sludge, which are suspected to lead to increased membrane fouling.

In addition to investigating the effect of temperature on membrane fouling, some studies also focused on the effect of SRT on membrane performance. Miyoshi et al., (2009) operated two separate MBRs with different SRTs during high- and low-temperature periods (10-22.6 $^{o}$C) to investigate seasonal variations in membrane performance. It was found that seasonal variations in membrane fouling were observed for the MBR with a shorter SRT (13 days). However, no fluctuations in membrane fouling were observed for the MBR with a longer SRT (50 days) suggesting that extending the SRT can possibly mitigate fluctuations in fouling due to seasonal variations in operating temperatures.

The effect of temperature on membrane performance was also investigated by Martín-Pascual et al., (2016). This study examined the influence of seasonal variations on the performance of UF membranes in a hybrid moving bed membrane bioreactor in a pilot-scale plant. The study did not only report that low-temperature operations correlate to higher fouling rates, it also found that the recovery of permeability after chemical cleaning was reduced under such conditions. The results of this study suggest that the recovery in membrane permeability with cleaning should also be investigated when evaluating the impact of seasonality on membrane performance.

## 2.2 Theories and mechanisms of fouling

The impact of seasonal variations on various operating conditions leading to increased membrane fouling was discussed in the previous section. There are many different theories on how changes in

various operating conditions can lead to increased membrane fouling in MBRs. The mechanisms at which MBR membranes foul under various operating conditions will be reviewed in the section below.

### 2.2.1 Effect of temperature on membrane foulants

The impact of cold water conditions on potential foulants in MBRs has been reported in several studies. Sun et al. (2014) and Ma et al. (2013) attributed increased fouling under low-temperature operations to the increase in the concentration of supernatant organics in the mixed liquor (humics, polysaccharides, and proteins). These organics are commonly referred to as soluble microbial products (SMPs) or EPS. Ma et al., (2013) observed that the alteration in foulants under cold water conditions was largely due to changes in the microbial community. At lower temperatures, higher fouling was attributed to the domination of filamentous bacterial communities. However, at higher temperature, Zoogloea was present, which was believed to have absorbed fine particles leading to a reduction in membrane fouling. On the other hand, Lyko et al. (2008) reported that while periods of low water temperatures corresponded to higher concentrations of biopolymers (carbohydrates and proteins) no correlation between carbohydrate concentrations and filterability was found. This was assumed to be due to other influencing parameters at the full-scale plant that prevented the observation of apparent correlations. This study concluded that soluble compounds are an inappropriate indicator of sludge filterability due to the complexity of the influencing phenomena. Therefore, there is a clear lack of consensus on increased organic matter being the cause of rapid deterioration in membrane performance under low-operating conditions.

Several other studies observed increased concentrations of organic matter in membrane feedwater under low-temperature operations. Van den Brink et al. (2011) and Wang et al. (2010) reported increased concentrations of EPS, polysaccharides, and proteins under temperature conditions ranging between 7-15$^{o}$C. Wang et al., (2010) found that the increase in these organics led to the attachment of biopolymers to membrane surfaces and in turn caused severe membrane fouling. This study concluded that the variation in feedwater characteristics due to seasonal fluctuations in temperature could be a result of increased production of biopolymers by the microbial community, as well as a reduction in degradation of organics. However, Rosenberger et al., (2006) and Gao et al., (2013) specifically attributed the increase in concentration of foulants under cold water operations to increased release by biomass. Rosenberger et al., (2006) demonstrated that the concentration of

organic matter was responsible for the differences in membrane performance, with high fouling rates corresponding to high polysaccharide concentrations in sludge supernatant. The study concluded that organics responsible for membrane fouling were of microbial origin produced under low-temperatures and stress situations. In contrast, Krezeminski et al. (2012) associated the increased fouling potential of membranes under low temperatures to the decrease in biological activity of biomass resulting in slower biodegradation of wastewater constituents. The results of this study showed a correlation between SMP and membrane resistance but no correlation was found between temperature and SMP concentration. Therefore, this study concluded that foulants arise from reduced hydrolysis and not release by biomass. Although both studies established that increased concentrations of organic matter in membrane feed led to higher fouling, both studies had different conclusions on the source of foulants.

### 2.2.2 Effect of solid residence time on membrane performance

The effect of SRT on membrane performance was reported in several studies. A study of the long- and short-term permeability evolution as a function of operational variables in a full-scale MBR was presented by Philippe et al., (2013). The study found that membrane fouling fluctuated seasonally due to changes in SRT. The relative importance of SRT on membrane performance was also observed by Miyoshi et al., (2009). This study focused on the development of reversible and irreversible fouling due to seasonal variations in operating conditions and found that fluctuations in membrane performance was only evident at low-SRT (13 days). However, in the MBR with long SRT (50 days), there were no significant seasonal variations in both types of membrane fouling. Al-Halbouni (2008) observed an increase in the concentration of polysaccharides and proteins during cold temperature periods, when the mixed liquor temperature ranged between 13-16$^{o}$C, in full-scale MBRs. The increase in supernatant organics corresponded with increased membrane fouling. This study found that the polysaccharides and proteins, which were involved in membrane fouling at lower SRT, were not detected in fouling layers at higher SRT. Therefore, since membrane fouling due to seasonal variations in operating conditions was found to be more evident at lower SRTs in several studies, it can be concluded that SRT plays a vital role in feedwater characteristics in MBRs and hence, membrane performance.

## 2.3 Research needs

The literature review revealed relatively little study of the fouling of tertiary membranes under stressed operating conditions. All studies that focused on the performance of tertiary membranes were conducted on a pilot or bench-scale indicating the need for full-scale studies. As was mentioned in the introduction, seasonal variations lead to fluctuations in flows, which can alter HRT or F/M ratio. However, as can be seen from the literature review, there is a lack in research studying the effect of fluctuations in raw wastewater flows on membrane fouling in terms of HRT and F/M in tertiary membranes.

The review revealed that there is a lack of consensus on the characteristics and source of foulants responsible for the deteriorations in performance of low-pressure membranes under stressed operating conditions (low-temperatures). Therefore, there is a need for a long-term characterization study of feedwater quality in a full-scale plant that spans multiple seasons of operation in order to elucidate the mechanisms responsible for fouling of tertiary membranes

# Chapter 3-Historical Analysis

## 3.1 Introduction

Membrane technologies are increasingly being employed in wastewater treatment in response to progressively more stringent regulations as well as a heightened interest in water reuse (Torà-Grau et al., 2014). They are typically incorporated into the treatment train either as part of a membrane bioreactor (MBR) or for tertiary filtration downstream of secondary treatment (Kent et al. 2011). However, the widespread application of this technology is somewhat limited by fouling that can lead to a decline in membrane permeability and overall performance (Ma et al. 2013). Fouling of membranes leads to the need for backwashing and chemical cleaning, thereby increasing the cost of operation and shortening lifespans (Abdullah and Bérubé 2013).

Membrane materials, feedwater characteristics, operational conditions and biomass characteristics have been found to influence the performance of membranes employed for wastewater applications (Meng et al., 2009; Sweity et al., 2011). In MBRs solids residence time (SRT) is also believed to have an effect on sludge properties that influence fouling (Al-Halbouni et al., 2008). Further, seasonal variations in operational conditions have been observed to influence membrane fouling in full-scale MBR systems (Rosenberger et al., 2006; Lyko et al., 2008; Wang et al., 2010b; Van der Brink et al., 2011). Seasonal fluctuations in raw wastewater temperature and flow can affect bioreactor performance and consequently the foulant characteristics in membrane feed streams. There are however few reports of the effect of seasonal variations on the fouling of tertiary membranes. The literature on membrane bioreactors operating under such conditions was reviewed to identify mechanisms that may impact tertiary membranes. While it is recognized that in MBRs the membranes are exposed to higher concentrations of suspended solids than tertiary membranes, it is believed that soluble- components would have a similar impact on membrane performance in both configurations.

Several studies of seasonal deterioration of membrane performance due to low operating temperatures have been reported (Sun et al., 2014, Al-Halbouni et al., 2008., Rosenberger et al., 2006, van der Brink et al., 2011). Fouling under low operating temperatures has been attributed to the presence of elevated concentrations of supernatant organics (humics, polysaccharides, and proteins) under such conditions. Sun et al. (2014) and Al-Halbouni (2008) observed an increase in the concentration of

supernatant organics (polysaccharides and proteins) during cold temperature periods, when the mixed liquor temperature ranged between 13-16$^{o}$C, in full-scale MBRs. In both cases, the increase in supernatant organics corresponded with increased membrane fouling. Van den Brink et al. (2011) and Wang et al. (2010) identified that the concentrations of extracellular polymeric substances (EPS), polysaccharides, and proteins increased under low-temperature conditions ranging between 7-15$^{o}$C. It was hypothesized that this lead to an increase of biopolymers attached to the membrane surfaces thereby causing enhanced fouling in pilot-scale MBRs. In contrast, Krezeminski et al. (2012) associated the increased fouling potential of membranes under low temperatures to the decrease in biological activity of biomass resulting in slower biodegradation of wastewater constituents.

Other studies have however suggested that mechanisms other than elevated foulant concentrations may be responsible for increased membrane fouling under cold water conditions. Differences in water viscosity with temperature (Sun et al., 2014; Ma et al., 2013) and reduced recovery of flux after membrane cleaning (Martín-Pascual et al., 2015) have also been implicated. Further, Lyko et al. (2008) reported that while periods of low water temperatures corresponded to higher concentrations of biopolymers (carbohydrates and proteins) no correlation between carbohydrate concentrations and filterability was found. This was assumed to be due to other influencing parameters at the full-scale plant that prevented the observation of apparent correlations. It is clear that further study is required to establish the relationship between seasonal variations in operating conditions and membrane fouling.

Tertiary ultrafiltration (UF) membranes are currently in use at the Keswick Water Pollution and Control Plant (WPCP) to treat municipal wastewater in the Region of York, Ontario, Canada. Substantial deterioration in the performance of the membranes, which are employed downstream of the activated sludge process has been consistently observed during the early spring period (March to May). This period is characterized by low wastewater temperatures and elevated flows. The Keswick WPCP was employed as a case study to obtain insight into the interaction between dynamic extreme operating conditions and membrane performance. The goal of the case study was to identify critical operating conditions (water temperature and feed flow) leading to the deterioration of membrane performance based on an analysis of historical data over a 2-year observation period (2016, 2017). It was expected that the results of this work would then inform more detailed studies which would explore fundamental mechanisms and foulant characteristics.

## 3.2 Materials and Methods

### 3.2.1 Full-Scale Membranes

The Keswick Water Pollution Control Plant was initially constructed in 1984 and in 2010 underwent major expansion to increase its design capacity to 18,000 $m^3$/d. In addition, the dual media tertiary filters were replaced with tertiary ultrafiltration membranes. The tertiary treatment at Keswick consists of a flocculation tank followed by micro-screens and five ultrafiltration membrane trains. Each membrane train consists of 6 cassettes with 48 modules in each cassette. The trains contain bundles of ZeeWeed hollow-fiber modules operating under negative pressure created within the hollow fibers by permeate pumps. The membranes remove relatively large particles, such as microbes, bacteria and macromolecules with molecular weights greater than about 300,000. The general process schematic of the Keswick WPCP can be found in Appendix B.

The UF trains are operated at a pre-determined production flow up to a maximum Trans-Membrane Pressure (TMP), or a minimum tank level. Treated water is periodically used to back-pulse (BP) the membranes to maintain stable TMP in the ultrafiltration trains. The membranes are also cleaned using maintenance cleans (MC) and recovery cleans (RC) to restore permeability. During both cleans the membranes are soaked in sodium hypochlorite or citric acid for 15 minutes for MCs, and 5 hours for RCs. The concentration of the cleaning chemical is typically higher in RCs (500 mg/L for Hypochlorite or 2000 mg/L for citric acid) than MCs (100 mg/L for Hypochlorite or 1000 mg/L for citric acid). Depending on plant demand, an ultrafiltration train proceeds to production and then back-pulse mode. This will continue until the permeate flow demand decreases, placing the train on standby. A train goes into MC or RC modes according to a set schedule, or when the membrane TMP is approaching its maximum value.

### 3.2.2 Data Mining

InSight, an Asset Performance Management (APM) tool created by Suez Water Technologies and Solutions, is used by the Keswick WPCP to provide real-time data on the performance of the membrane trains. InSight is employed to visualize key performance indicators (KPIs) before, after and during back-pulses. A correction factor (TC Factor) is used to correct permeability, flux, and TMP for changes in water viscosity with temperature. At the Keswick WPCP information on various membrane operating parameters are collected at different frequencies. A list of the main train

operational parameters, their frequencies and units, which are available on Keswick's InSight platform, are presented in Table 1.

**Table 1-InSight platform operational parameters**

| Parameter | Frequency | Unit |
|---|---|---|
| Flow Rate Before/After/ During BP | Every BP | $m^3/hr$ |
| Flux Before/After/During BP | Every BP | Lmh |
| Permeability Before/After/During BP | Every BP | Lmh/bar |
| Temperature Corrected (TC) Flux Before/After/During BP | Every BP | Lmh |
| TC Permeability (TCP) Before/After/During BP | Every BP | Lmh/bar |
| TMP Before/After/During BP | Every BP | kPa |
| TC-TMP Before/After/During BP | Every BP | kPa |
| Maintenance and Recovery Clean Types | Per clean | - |
| Total Wastewater Feed Flow | Daily | $m^3$ |
| Train Mode | 1-minute | - |
| Permeate Temperature | 15-min | $^oC$ |
| Permeate Turbidity | 15-min | NTU |

Building on the data gathered by the Insight platform a detailed historical analysis of membrane operations was conducted to obtain a comprehensive understanding of membrane fouling over time at the Keswick facility. The historical analysis characterized fouling between consecutive back-pulses, RCs and MCs, and also quantified the reclamation of permeability that was achieved in the various cleaning processes. In this study, a cycle was defined as the production period between two successive back-pulses. A fouling index (FI) was calculated for each cycle for two representative trains (UF1 and UF4) for the years of 2016 and 2017 using Equation 1:

$$FI = \frac{P(A_N) - P(B_{N+1})}{\Delta t} \quad (1)$$

Where: $P(A_N)$*: TCP after back-pulse (Lmh/bar)*

$P(B_{N+1})$*: TCP before next back-pulse (Lmh/bar)*

$\Delta t$*: Length of permeation between successive BP (minute)*

Fouling slopes (FS) were calculated to quantify fouling between two consecutive MCs and RCs using Equation 2. For all calculations involving MCs or RCs, the TCP during BP was used to capture the change in permeability as flux is only consistent during BPs, and TCP data in terms of MCs or RCs are not available.

$$FS = \frac{P\left(D_{N+1\,(C)}\right) - P\left(D_{N-1\,(C+1)}\right)}{\Delta t} \quad (2)$$

Where: $P(D_{N+1\,(C)})$*: TCP during BP for initial BP after MC or RC (Lmh/bar)*

$P(D_{N-1\,(C+1)})$*: TCP during BP for the last BP before MC or RC (Lmh/bar)*

$\Delta t$*: Length of permeation between successive MCs or RCs (minute)*

To determine if the recovery in permeability after membrane cleans was affected by the operational conditions, the reclamation of permeability was calculated for back-pulses, MCs and RCs using Equations 3-4 respectively:

$$R_{BP} = P(A_N) - P(B_N) \quad (3)$$

Where: $P(A_N)$*: TCP after back-pulse*

$P(B_N)$*: TCP before back-pulse*

$$R_c = P(D_{N+1\,(C)}) - P(D_{N-1\,(C)}) \quad (4)$$

Where: $P(D_{N+1\,(C)})$*: TCP during BP for BP immediately after MC or RC*

$P(D_{N-1\,(C)})$*: TCP during BP for BP immediately before MC or RC*

Metastatistics on the calculated parameters are displayed in Table 2. Data describing the permeate temperature and raw wastewater daily flow were also collected for the study period.

**Table 2-Number of data points calculated for this study**

| Parameter | Number |
|---|---|
| Fouling indexes for permeation cycles | 6593 |
| Fouling slopes MC | 569 |
| Fouling slopes RC | 59 |
| Reclamation BP | 7371 |
| Reclamation MC | 509 |
| Reclamation RC | 65 |

As mentioned previously, the trains were not continuously in production mode and the InSight platform therefore records the operational status of each train on a 1-minute basis. Train status codes that are employed by Insight are summarized in Table 3. To determine the length of permeation within a cycle, MATLAB- R2018a was used to count the number of production codes (13XX) between two back-pulses (34XX). MATLAB was also used to calculate FI values for each cycle as per Equation 3. The same technique was used to determine the fouling slopes between two MCs and RCs, as MATLAB was used to count the number of production codes between two MCs (58XX) and RCs (85XX). MATLAB was further used to estimate the permeate temperature during a specific cycle based on the temperature data values available in InSight, that were recorded every 15 minutes. The scripts used to correct for data time-lags and calculate all parameters using equations 1-4 are available in Appendix C.

**Table 3-Train status codes**

| Train Status | Code |
|---|---|
| Standby | 5XX |
| Production | 13XX |
| Back-pulse | 34XX |
| Maintenance Clean | 58XX |
| Recovery Clean | 85XX |
| Shutdown | 2XX |

## 3.3 Results

### 3.3.1 Fouling Index

The fouling index metric was employed in this study for each cycle to represent the rate of deterioration of membrane permeability per unit time of production. Sun et al. (2014), and Ma et al. (2013) suggested that the rapid decline in permeability during cold water periods is a result of changes in water viscosity with temperature. Hence, the temperature corrected permeability was used in the current study to account for changes in viscosity. The fouling indexes for trains UF1 and UF4 that were calculated for the years of 2016 and 2017 are plotted in Figures 1 and 2 respectively. From these figures it can be seen that both trains behaved similarly in a given year indicating that fouling behavior of the membranes was independent of the train used.

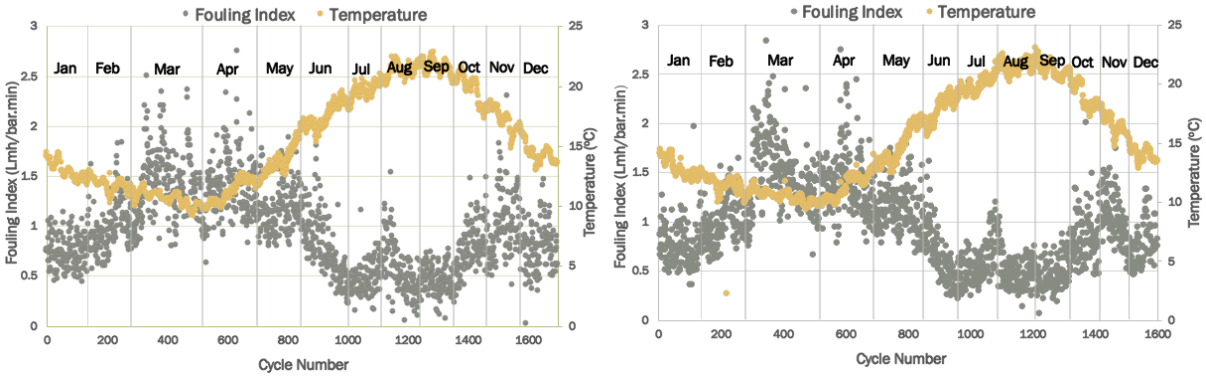


**Figure 1- Fouling indexes and temperature for UF1 (left) and UF4 (right) for 2016**

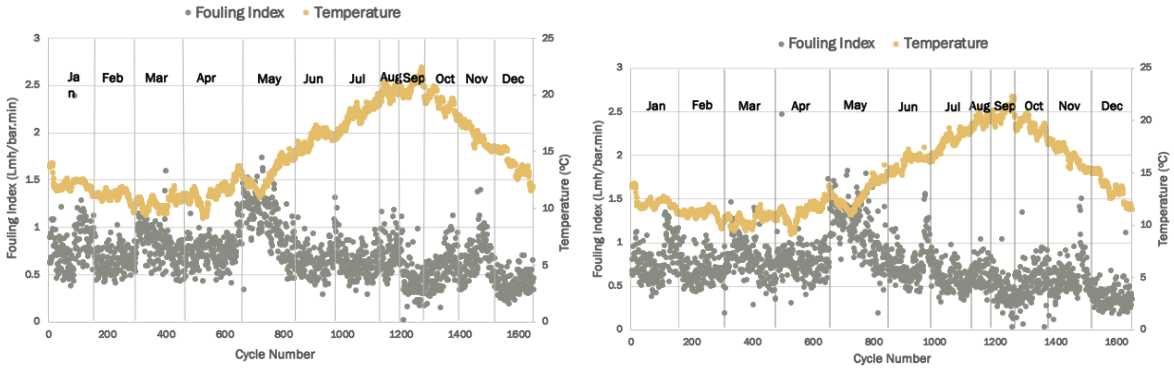


**Figure 2-Fouling indexes and temperature for UF1 (left) and UF4 (right) for 2017**

It was initially anticipated that the fouling responses would have similar seasonal patterns for each year. From Figure 1 it can be seen that for the year 2016, elevated fouling indexes were observed

during March and April. However, as can be seen in Figure 2, this was not the case for 2017 as the fouling index fluctuated up and down over the period between January and May. The differing patterns suggested a more complex dependence of fouling on the operating conditions.

The difference in fouling behavior between the two study years was investigated by examining trends in permeate temperature and wastewater flow. As can be seen in Figure 1, for 2016, the water temperature was generally lower in March and April, ranging between 9-13 $^{o}$C, during high fouling periods that were defined as having an average FI of 1.42 Lmh/bar.min. The average FI values were calculated by averaging the FI values of all cycles in March and April of 2016 for UF1 and UF4. The water temperature was higher, ranging between 15-23 $^{o}$C, during periods of low fouling (June-November) as defined by an average fouling index of 0.67 Lmh/bar.min. The relationship between temperature and fouling index values differed in 2017 as can be seen in Figure 2. The water temperature dropped to a low range of 9-13 $^{o}$C between February and April and reached a high range of 15-23 $^{o}$C between September and November. However, this temperature pattern did not correspond to the same response in fouling index as observed in 2016. In 2017, the fouling index tended to fluctuate somewhat randomly while the pattern in water temperature was relatively consistent between the two years.

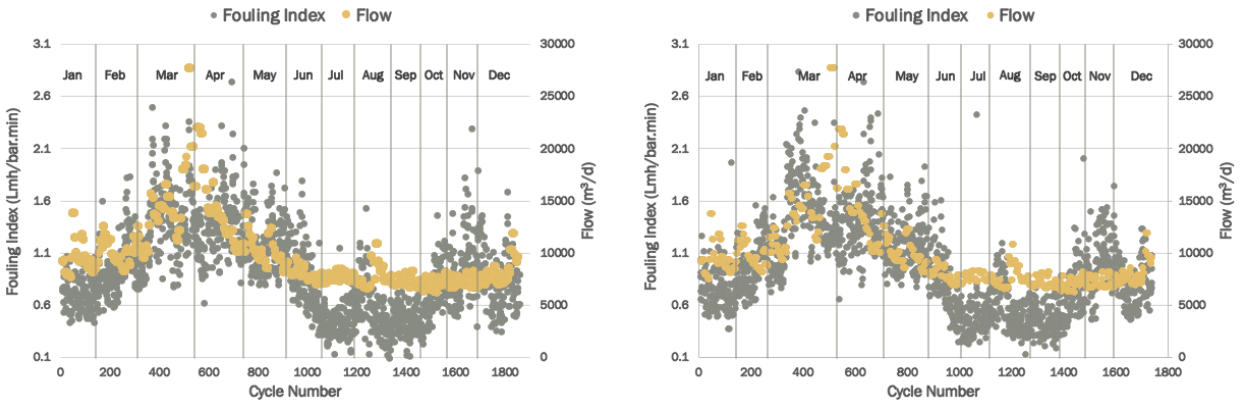


**Figure 3-Fouling indexes and wastewater flow for UF1 (left) and UF4 (right) for 2016**

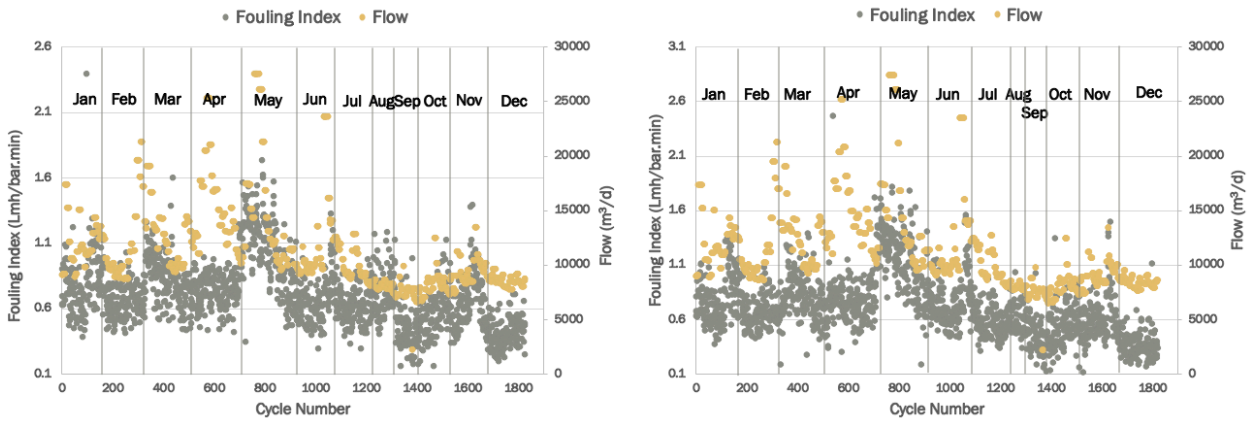


**Figure 4-Fouling indexes and wastewater flow for UF1 (left) and UF4 (right) for 2017**

The FI values were plotted against the total wastewater daily flow for each year to assess whether there were any relationships between these parameters. It was hypothesized that the HRT in the upstream activated sludge process might impact on the presence of foulants in the membrane influent. As can be seen in Figure 3, for 2016, wastewater flow values were highest, ranging between 10,000-27,700 $m^3$ per day, during the high fouling period between March and April (average FI of 1.42 Lmh/bar.min). The wastewater flow remained relatively consistent, ranging between 6000-10000 $m^3$ per day, between June and November, which was the period marked by lower FI values with an average of 0.67 Lmh/bar.min. For 2017, the flow randomly fluctuated throughout the year, reaching its highest values (average flow of 15150 $m^3$/day) during May, which coincided with more intensive fouling with an average FI value of 1.06 Lmh/bar.min. The lowest fouling rates occurred between September and December, with average FI values of 0.48 Lmh/bar.min and average flow of 7808 $m^3$/day.

### 3.3.2 Fouling between MCs and RCs

The fouling slopes between successive MCs and RCs were calculated to describe the rate of membrane performance deterioration between cleans. As can be seen in Figure 5, during the year of 2016, the fouling slopes between MCs and RCs were highest for March and April. This pattern coincided with that described in the previous section, with the highest in-cycle fouling occurring during March and April in 2016. For the year of 2017 (Figure 6) the highest fouling slopes between cleans persisted between January and May as was also observed for the in-cycle fouling between BPs.

The similar fouling patterns suggested that fouling was independent of cleaning type, as deterioration of membrane permeability between BPs, MCs, and RCs occurred around the same time each year.

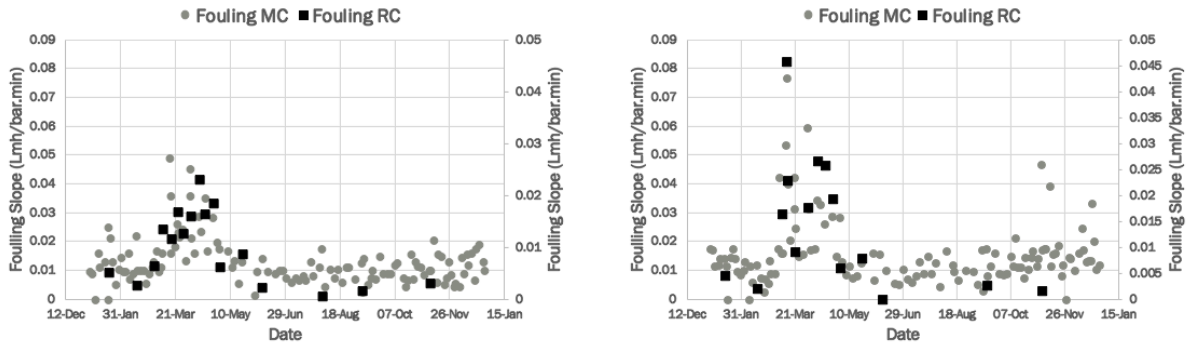


**Figure 5-Fouling slopes between MCs and RCs for 2016 UF1 (left) and UF4 (right)**

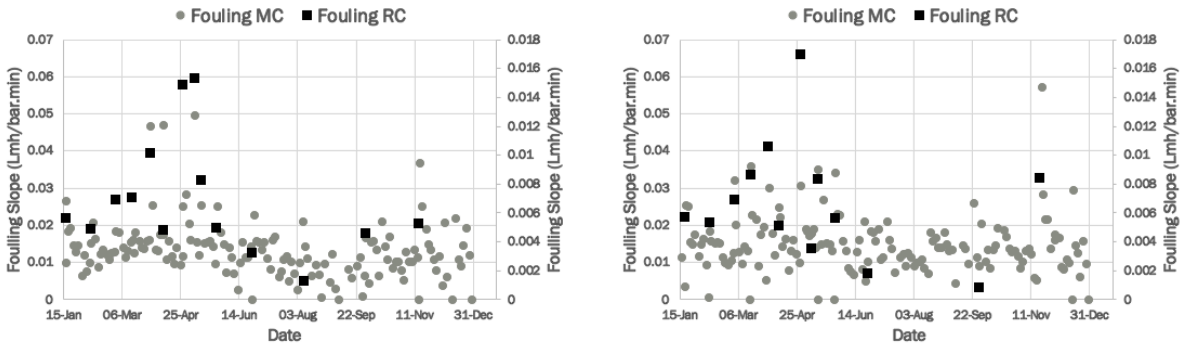


**Figure 6-Fouling slopes between MCs and RCs for 2017 UF1 (left) and UF4 (right)**

### 3.3.3 Permeability Reclamation

Previous studies have implied that poor membrane performance might result from a reduction in the recovery of flux after membrane cleaning (Martín-Pascual et al.,2016). A reduction in the effectiveness of a membrane clean can result in poor filterability during the following cycle. To investigate the possibility of this being the cause of increased fouling during extreme weather events, the reclamation of permeability due to BPs, MCs, and RCs was plotted in Figures 7-10 respectively. As can be seen in Figure 7, in 2016, permeability reclamation values due to back-pulsing were highest between March and May. As previously discussed, in 2016, March and April marked the period of highest fouling. When the FI and reclamation results were examined collectively it is

evident that more permeability was recovered due to back-pulsing during periods of higher fouling. In 2017 (Figure 8) the highest reclamation of permeability also occurred during periods of higher fouling which were distributed between January and May.

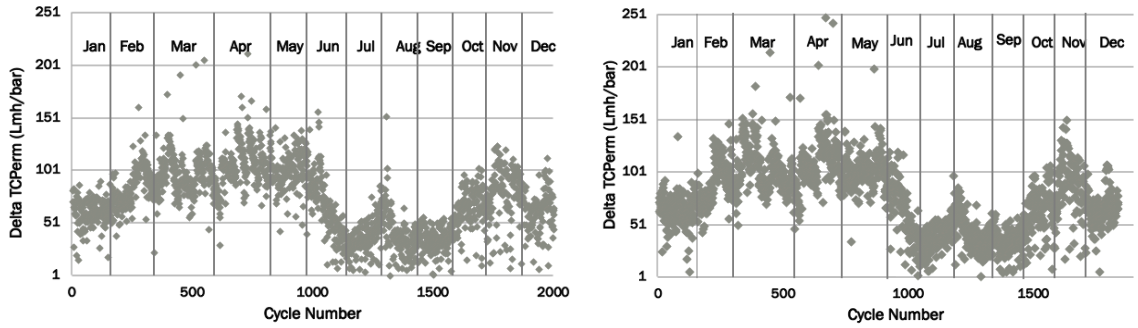


**Figure 7-Permeability reclamation due to BP for 2016 UF1 (left) and UF4 (right)**

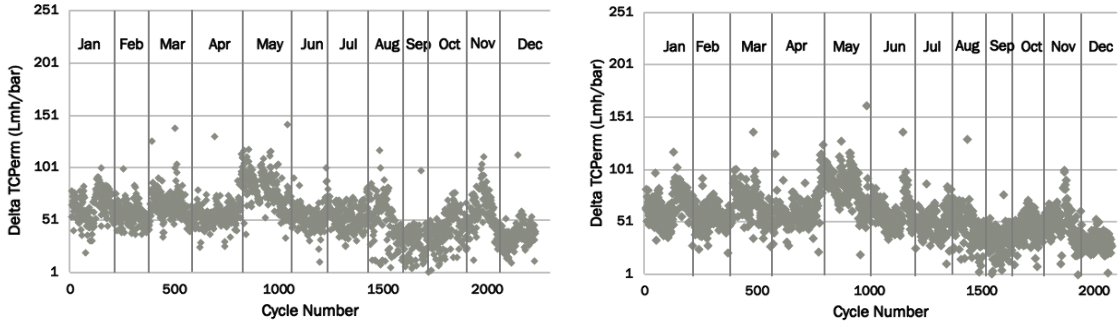


**Figure 8-Permeability reclamation due to BP for 2017 UF1 (left) and UF4 (right)**

Similar conclusions were arrived at when the reclamation in permeability after MCs and RCs was examined. As can be seen in Figure 9, the highest recovery in membrane permeability due to MCs and RCs occurred during March and April in 2016. In 2017 (Figure 10) the highest reclamation values were observed between January and May. The results suggest that the deterioration in membrane performance did not result from a decrease in the effectiveness of the membrane cleans, as the reclamation of permeability was found to increase during high fouling periods.

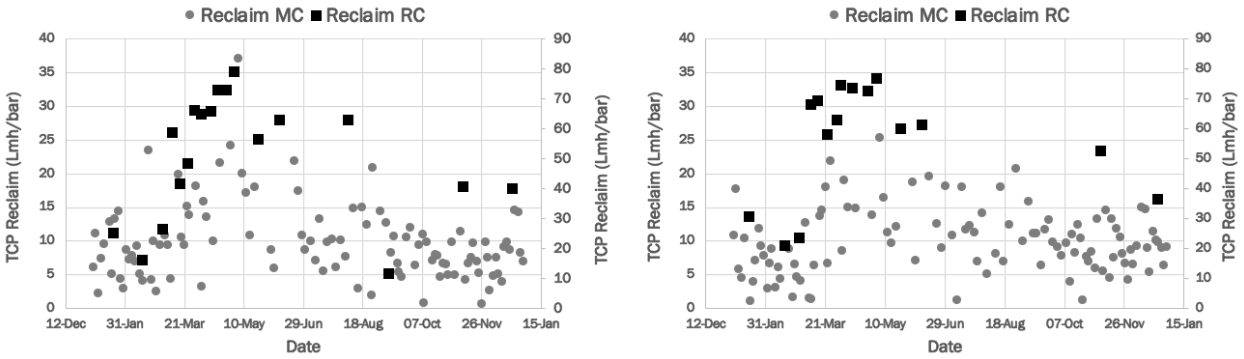


**Figure 9- Permeability reclamation due to MC and RC for 2016 UF1(left) and UF4(right)**

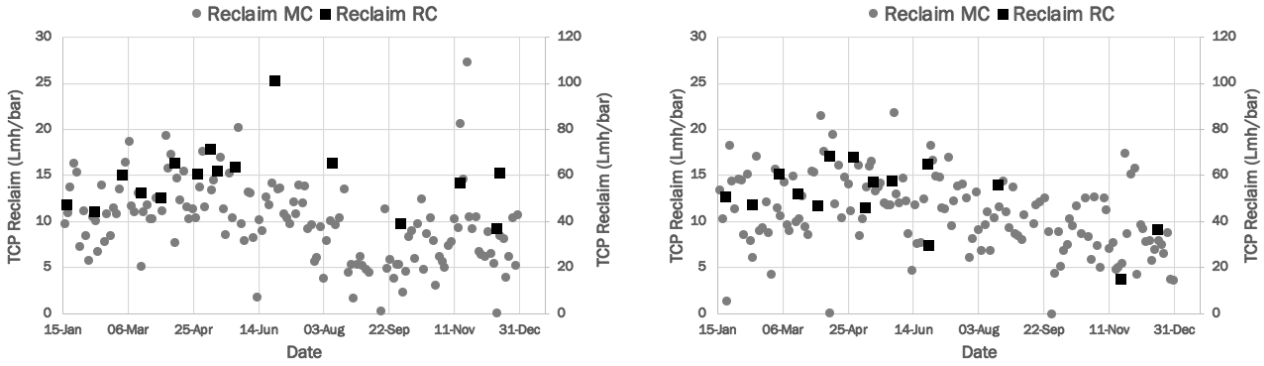


**Figure 10-Permeability reclamation due to MC and RC for 2017 UF1(left) and UF4(right)**

Based on the results of this study, it was evident that there was a relationship between deterioration in membrane performance and water temperature and flow. These impacts were greater than that which would be expected from changes in water viscosity with temperature and could not be explained by reduced cleaning performance under these conditions. The effect of temperature on fouling in MBRs has been attributed to increases in supernatant organics (polysaccharides and proteins) in the membrane feed (Sun et al. 2014; Al-Halbouni et al. 2008; Rosenberger et al. 2006; van den Brink et al. 2011) under low temperature operation. However, the effect of dynamic changes in wastewater flow on fouling of this nature has received less attention. Lyko et al. (2008) reported that significant variations in the raw wastewater inflow resulted in changes in the food to microorganism ratio (F/M) while Kimura et al. (2005) have observed that deviations in the F/M ratio of MBRs were a major contributor to alterations to the nature of foulants. Hence, the results of this study were consistent with the MBR literature which has suggested that both temperature and flow may affect membrane performance by influencing upstream activated sludge processes which alter foulant characteristics of

the membrane feed. Prior studies on the combined impacts of varying temperature and flow have however not been reported and hence additional characterization of these effects was performed in this study.

To determine the significance of each variable (temperature and flow) independently on overall fouling, a multivariate linear regression analysis was conducted using Microsoft Excel. Linear regression analysis is commonly used to uncover the relationship of one variable to a number of independent variables (Jones, 1972). Microsoft Excel regression analysis function uses the "least squares" method to perform linear regression. However, the lease-squares estimate of regression coefficients can become highly inaccurate if the independent variables are correlated (Jones, 1972). In order to determine whether there is a relationship between temperature and flow, Microsoft Excel's function CORREL was used. This function returns the correlation coefficient between two arrays of data using Equation 5. A correlation coefficient of +1 indicates a strong positive correlation, while a coefficient of -1 indicates a strong negative correlation.

$$Correl(X,Y) = \frac{\sum(x-\bar{x})(y-\bar{y})}{\sqrt{\sum(x-\bar{x})^2 \sum(y-\bar{y})^2}} \quad (5)$$

Where: $\bar{x}$ *and* $\bar{y}$ *are the sample means of array* $X$ *and* $Y$

Using this function, a correlation coefficient of -0.6164 was determined suggesting a negative correlation between water temperature and flow. Hence, it was not possible to directly attribute the observed changes in fouling to either the higher flows or lower temperatures. Tests that include independent control of temperature and flow would be required to delineate the relative contribution of these variables to fouling.

In several recent studies low SRT have been reported to have a negative impact on fouling through increases in EPS and soluble microbial products (SMP) (Ahmed et al., 2007; Liang et al., 2007, Masse´ et al., 2006; Al.Halbouni el al., 2008). However, in the current study SRT was controlled within a relatively narrow range by the plant operators (Figure 11). As can be seen in Figure 11, the plant's SRT remained predominantly consistent during each year, with a slight increase in values during the cold water periods (January- April and November-December). The high fouling periods of 2016 and 2017 are marked with vertical lines on Figure 11. As can be seen in the figure, SRT values did not follow any pattern during high fouling periods in comparison to the rest of year during the

study. Therefore, the effect of SRT on fouling of the membranes at Keswick was discounted in this study.

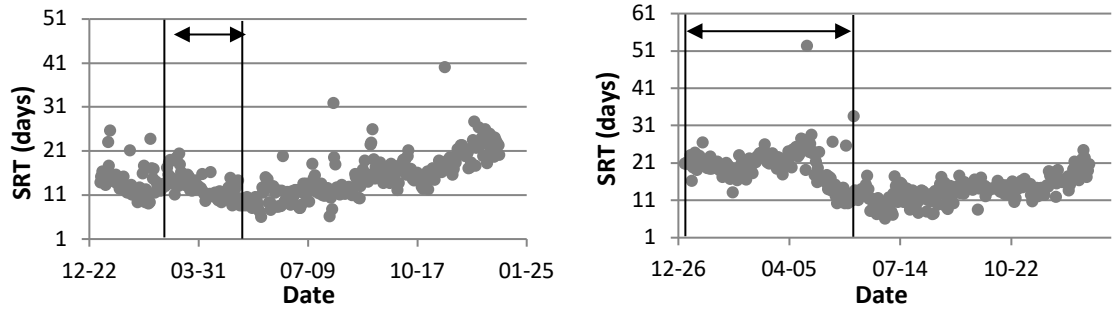


**Figure 11-SRT values for the years 2016 (left) and 2017 (right)**

## 3.4 Conclusions and Recommendations

The effect of seasonal variations in operating conditions (temperature and flow) on membrane performance was studied in full-scale tertiary membranes treating domestic wastewater for a period of 2-years. The fouling behavior of parallel membrane trains (UF1 and UF4) were nearly identical during the two year observation period, indicating that fouling is independent of train used. It was observed that the membrane fouling behavior significantly differed between the two year-long observation periods, with a peak in fouling indexes during March and April for 2016, and inconsistent fluctuations in fouling indexes between January and May for 2017. The differing patterns suggested a more complex dependence of fouling on the operating conditions. The reclamation of permeability as a result of membrane back-pulses and cleans increased during high fouling periods, indicating that the deterioration in membrane performance did not result from a decrease in the effectiveness of membrane cleans. A relationship was observed between the deterioration in membrane performance and water temperature and flow and this was more than could be explained by changes in water viscosity with temperature. The results suggest that membrane performance is influenced by both of these seasonal variations in operating conditions that impact the upstream activated sludge process. However, it was not possible to delineate the contributions of the individual variables as they were found to be highly correlated.

# Chapter 4- Foulant Characterization

## 4.1 Introduction

The need for improved treated wastewater quality has led to upgrading of wastewater treatment plants through the addition of tertiary treatment. Membrane technologies are increasingly being employed in this regard to meet stringent regulations on suspended solids and pathogen concentrations, often in support of water reuse initiatives (Torà-Grau et al., 2014). Membranes are typically incorporated in the treatment train downstream of activated sludge or as membrane bioreactors (MBRs) (Kent et al., 2011). Although this technology has proven useful in producing high-quality effluent, membrane fouling has limited its widespread use as this leads to increased operational costs and a decline in overall performance (Ma et al. 2013). Increased fouling leads to the need for membrane cleaning, which requires the use of chemicals, increasing costs of operation and shortening membrane lifespan (Abdullah and Bérubé, 2013).

Membrane materials, feedwater characteristics, operational conditions and biomass characteristics have been reported to influence the performance of membranes employed for wastewater applications (Meng et al., 2009; Sweity et al., 2011). Further, seasonal variations in raw wastewater temperature and flow have been observed to affect bioreactor performance and consequently foulant characteristics in the membrane feed (Abu-Obaid, 2018). Abu-Obaid (2018) observed a relationship between the deterioration of membrane performance and variations in water temperatures and flows in full-scale tertiary membranes. Prior research has focused on the effect of operating conditions on the composition and filtration behavior of the mixed liquor impacting on the membranes in MBRs (Al-Halbouni et al., 2008, Lyko et al., 2008, Ma et al., 2013, Gao et al., 2013, Diaz et al., 2016). However, there are few reports of the effect of operating conditions on foulant composition and filtration behavior in tertiary membranes.

The impact of cold water conditions on membrane feedwater characteristics and sludge properties in MBRs have been reported. Sun et al. (2014) and Ma et al. (2013) observed an increase in the concentration of organics in the mixed liquor supernatant (humics, polysaccharides, and proteins) under such conditions. These organics are commonly referred to as soluble microbial products (SMPs) or extracellular polymeric substances (EPS). Al-Halbouni (2008) also observed an increase in the concentration of polysaccharides and proteins during cold temperature periods, when the mixed

liquor temperature ranged between 13-16$^{o}$C, in full-scale MBRs. The increase in supernatant organics corresponded with increased membrane fouling. Van den Brink et al. (2011) and Wang et al. (2010) reported increased concentrations of EPS, polysaccharides, and proteins under low-temperature conditions ranging between 7-15$^{o}$C. It has been hypothesized that these organics may arise from either reduced hydrolysis of potential foulants from influent wastewater (Krzeminski et al., 2011) or increased release by biomass under low-temperature conditions (Gao et al., 2013). Drew et al. (2007) observed that sudden temperature changes have a greater impact on SMP concentrations than steady state operation at low temperatures however it was not elucidated which mechanism was active in this study.

The operation of MBRs under cold water conditions has been found to lead to changes in sludge characteristics. Lyko et al. (2007) showed that temperature impacted the mixed liquor carbohydrate concentration and this was related to changes in sludge dewaterability. Al-Halbouni (2008) observed a negative impact on sludge dewaterability with an increase of soluble EPS concertation. Further, Le-Clech et al. (2006) revealed a direct relationship between soluble carbohydrates, fouling rates, and capillary suction time (CST). The results of these studies highlight the value of monitoring sludge properties when studying the effects of seasonal variation on fouling of tertiary membranes as it might be expected that components (primarily soluble) released from the activated sludge process would impact on the downstream membranes.

The membranes in MBRs interact with a range of potential foulants that span from truly soluble species to suspended solids, such as flocs (Rosenberger et al., 2006). It can be anticipated that tertiary membranes, which are not as exposed to settleable components, will have different fouling mechanisms, and therefore, may be differently affected by operating conditions. Hence, the current study focused on factors affecting fouling of tertiary membranes.

Tertiary ultrafiltration is currently used at the Keswick Water Pollution and Control Plant (WPCP) in the Region of York, Ontario, Canada. The plant treats an average of 18,000 $m^3$/d of domestic wastewater. A substantial deterioration in the performance of the membranes has been reported during the early spring period (March to May) (Abu-Obaid, 2018). The current study examined changes in foulant characteristics during high fouling events over a 17-month period to obtain an

improved understanding of the foulant characteristics under the challenging conditions of low temperature and elevated wastewater flows.

## 4.2 Materials and Methods

### 4.2.1 Full-Scale Membranes

The Keswick Water Pollution Control Plant (WPCP) located in the Regional Municipality of York was initially constructed in 1984 and in 2010 underwent major expansion increasing its capacity to treat an average flow of 18,000 $m^3$/d and replacing dual media tertiary filters with tertiary ultrafiltration. The tertiary treatment at Keswick consists of a flocculation tank followed by micro-screens and five ultrafiltration membrane trains. The UF units employ ZeeWeed hollow fiber modules suspended in the feedwater, and operating under negative pressure created within the hollow fibers by permeate pumps.

The UF trains are operated at a pre-determined production flow up to a maximum Trans-Membrane Pressure (TMP), or a minimum tank level. Treated water is periodically used to back-pulse (BP) the membranes to maintain stable TMP in the ultrafiltration trains. The membranes are also cleaned using maintenance cleans (MC) and recovery cleans (RC) to restore permeability. During both cleans the membranes are soaked in sodium hypochlorite, citric acid or hydrochloric acid for 15 minutes for MCs, and 5 hours for RCs. Depending on plant demand, an ultrafiltration train proceeds to production and then back-pulse mode. This will continue until the permeate flow demand decreases, placing the train on standby. A train goes into MC or RC modes according to a set schedule, or when the membrane TMP is approaching its maximum value.

### 4.2.2 Sampling

The impact of seasonal variation of operating conditions on fouling behavior and foulant characteristics was assessed by collecting and characterizing samples of the membrane feedwater over an extended period of time. The sampling programme was developed to generate data on potential foulants on an increased frequency during periods of high fouling and reduced frequency during low fouling periods to conserve resources. In this regard, triplicate grab samples were collected from the effluent of the micro-screens, which was the influent to the UF membranes, on a weekly basis between January-May 2017 (cold weather). The sampling frequency was then reduced to once per month during the subsequent warm weather period to develop a baseline of operations

during warm weather. The sampling frequency reverted back to a weekly basis between January-May 2018 to obtain a detailed characterization of fouling under the second cold weather period.

Samples of additional process streams were collected to gain further insight into potential causes of fouling. In this regard, triplicate samples of the raw wastewater entering the plant were collected between October 2017 and May 2018 to help identify the source of foulants. Samples were collected once per month between October and December 2017, then biweekly for the remaining months (January- May 2018). In addition, duplicate grab samples of the mixed liquor from the plant's North and South aeration basins were collected at the same frequency as membrane feed, to gain insight into sludge characteristic changes during the study.

### 4.2.3 Membrane Feed Characterization

Samples of the membrane feedwater were characterized with respect to water quality parameters that were anticipated to have potential impacts on membrane permeability (Table 4). Saravia et al. (2006) revealed a significant influence of ionic strength, especially of calcium ions, on the permeability of membranes in an MBR. Hence, the concentrations of various cation, and anions species were measured for this study. Nitrogen species concentrations were also measured as they were considered to be indicators of the state of the biological process. The remaining parameters (TOC, DOC, cBOD5, COD, Turbidity) were included as measures of colloidal and dissolved organic matter which are suspected to foul UF membranes (Citulski et al., 2009)

**Table 4-Water quality parameters measured**

| Parameter | Units |
|---|---|
| pH | - |
| Conductivity | µS/cm |
| Temperature | $^{o}$C |
| Turbidity | NTU |
| Total organic carbon (TOC) | mg/L |
| Dissolved organic carbon (DOC) | mg/L |
| Carbonaceous biological oxygen demand ($cBOD_5$) | mg/L |
| Chemical oxygen demand (COD) | mg/L |
| Dissolved organic nitrogen (DON) | mg/L |
| Cation concentrations ($Ca^{+}$, $Mg^{+2}$, $K^{+}$, $Na^{+}$) | mg/L |
| Anion concentrations ($Br^{-}$, $Cl^{-}$, $Fl^{-}$, $SO_4^{-}$, P) | mg/L |
| Nitrogen species concentrations -Ammonia and $NH_4$, Nitrate, Nitrite, total Kjeldahl nitrogen (TKN) | mg/L |

The water quality parameters described in Table 4 were analyzed by the York-Durham Regional Environmental Laboratory as per Standard Methods (APHA, 2017). Samples were transported on ice to the lab. Temperature, pH and turbidity were measured on site using HACH probes.

Membrane feedwater samples were also transported to the University of Waterloo for further testing. In prior studies of membrane fouling in drinking water applications, it was found that biopolymers, which consist of polysaccharides, proteins and protein-like substances, were the fraction of dissolved natural organic matter (NOM) which contributed to fouling of low-pressure membranes (Croft, 2012). Hence, the samples collected from the Keswick WPCP were analyzed for these sub-fractions and others, using an advanced analytical methodology which employs a Liquid Chromatograph coupled to Organic Carbon Detection (LC-OCD) (Huber et al. 2011). Samples were filtered through 0.45µm PES filters within 24 hrs of sampling and stored at a temperature of 4$^{o}$C before processing, which was generally conducted within 48 hrs of sampling.

LC-OCD is a form of high-performance size exclusion chromatography (HP-SEC) developed by Huber and Frimmel (1991). LC-OCD separates molecules based on their molecular weight/size,

shape, and interaction characteristics with large molecules eluting faster than smaller molecules. A sample volume of 1 mL was injected into the buffer solution (Phosphate buffer with a pH of 6.58) that formed the mobile phase which passed through the stationary column for molecule separation. The stationary SEC column was coupled with organic carbon and UV detectors. Based upon the shape of the detector response curves the DOM is separated into biopolymers (BP), humic substances, building blocks, low molecular weight (LMW) acids and neutral fractions (Lankes et al. 2009).

### 4.2.4 Determination of Mixed Liquor Dewaterability

The presence of EPS in mixed liquor has been observed to affect sludge dewaterability (Al-Halbouni et al., 2008). Hence, in the current study the mixed liquor dewaterability was characterized using the CST method to obtain an indirect measure of changes in floc properties that may have resulted from changes in EPS content. A Triton Electronics Ltd. Type 304M capillary suction test analyzer was used for this study. The CST method measures the time required for filtrate to wick out of a sample and to seep through a fixed distance of filter paper (Chen et al., 1996) and hence large CST values are indicative of poor sludge dewaterability.

### 4.2.5 Membrane Fouling Index

InSight, an Asset Performance Management (APM) tool created by Suez Water Technologies and Solutions, is used by the Keswick WPCP to provide real-time data on the performance of the membrane trains. InSight is employed to visualize key performance indicators (KPIs) before, after and during back-pulses. A temperature correction factor (TC Factor) is used to correct permeability to changes in water viscosity with temperature. Abu-Obaid (2018) employed various parameters on the Keswick Insight platform to quantify fouling between back-pulses, MCs and RCs. The parameters available on the platform were also used to quantify recovery in permeability after each cleaning type. For this study, the fouling index (FI) was employed to quantify the rate of deterioration of membrane permeability per unit time of production within a cycle. A cycle was defined as the production period between two successive back-pulses. The fouling index was calculated using Equation 6:

$$FI = \frac{P(A_N) - P(B_{N+1})}{\Delta t} \quad (6)$$

Where: $P(A_N)$*: TC-Permeability immediately after back-pulse (Lmh/bar)*

$P(B_{N+1})$*: TC-Permeability immediately before subsequent back-pulse (Lmh/bar)*

$\Delta t$*: Length of permeation between two BPs (minute)*

An average of the fouling index metric for each sampling day was calculated to quantify the fouling intensity for that day. The FI values were then compared with the measured values of the hypothesized membrane foulants to obtain insight into the underlying causes of the fouling.

## 4.3 Results

### 4.3.1 Variation in Feedwater Characteristics

A historical review of Keswick's membrane operational data concluded that membrane fouling was affected by alterations in foulant characteristics which resulted from the impacts of seasonal variations in water temperature and flow on the upstream biological processes (Abu-Obaid, 2018). Hence, the current study sought to identify the foulants responsible for the seasonal changes in fouling. This involved gathering data on conventional and unconventional water quality parameters over a period of 17-months. The data gathered with respect to conventional water quality parameters for the membrane influent over this period are presented in Figure 12. Vertical lines on the figure delineate periods which were previously identified as having high fouling. However, through the visual inspection of the figure, there appeared to be no clear pattern in parameters presented during high fouling period. Hence, for each sampling day, a fouling index was calculated by averaging the fouling indexes over all cycles that occurred that day. Fouling index values were then plotted against the various water quality parameters such as pH, conductivity, turbidity, $UV_{254}$, TOC/DOC, $cBOD_5$, COD, DON, several cation, anion, and nitrogen species concentrations to evaluate potential dependencies of fouling on water quality. Linear, logarithmic, polynomial, and power trendlines were developed for each parameter to assist with determining which characteristics had the highest influence on fouling index. It was found that there were only modest differences in the $r^2$ values when comparing the different statistical fitting models. Hence, the linear model was chosen to describe the relationship between the significant parameters and fouling index. Any relations leading to an r-squared value lower than 0.2 and a P-value higher than 0.05 were deemed to be statistically

insignificant. The r-squared, and P-values of each parameter measured in descending order, are presented in the supplementary material.

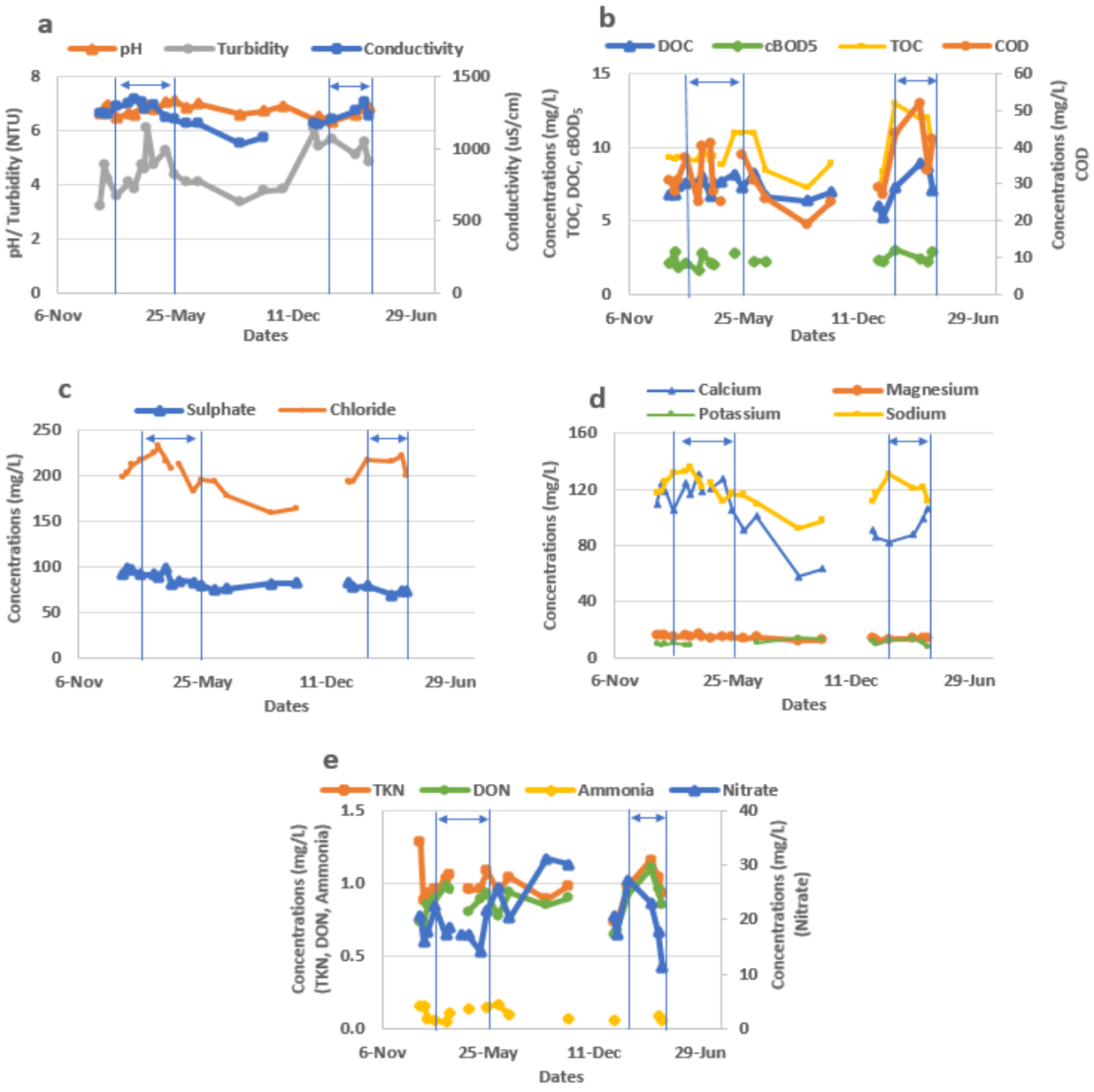


**Figure 12-Conventional water quality parameter responses versus time. a) pH, turbidity & conductivity, b)TOC, DOC, cBOD$_5$ & COD, c) anions, d)cations, e)nitrogen species. Vertical lines on the figures delineate periods of high fouling**

The highest correlations were observed between fouling index and TOC, DOC, and nitrate with $r^2$ values of 0.4192, 0.2785, and 0.2123 respectively, and $P < 0.05$ (Figure 13). A positive correlation was observed between fouling index, TOC, and DOC, with an increase in FI as the concentrations of TOC and DOC increased. However, a negative correlation was observed between fouling index and nitrate, with a decrease in FI as nitrate concentrations increased. There was considerable scatter around the regression lines but the residuals were randomly distributed and hence it was concluded that the linear regression relationship was able to describe the phenomena. In order to compare the relative importance of each independent variable deemed significant on fouling index, the variable inputs were standardized using Equation 7 and an equation for the linear regression line was determined for each using Microsoft Excel's Regression tool.

$$x_s = \frac{x - Min(X)}{Max(X) - Min(X)} \quad (7)$$

Where: $x_s$: *The standardized independent variable (x)*

$Min\ (X)$: *The smallest value in the X array*

*Max (X): The largest value in the X array*

The standardization of the variables was necessary to compare the absolute value of the slopes of each regression model on the same scale, as the variables spanned different magnitudes. The estimated confidence interval of each slope, which was calculated by adding and subtracting the standard error to the point estimates, are plotted in Figure 14.

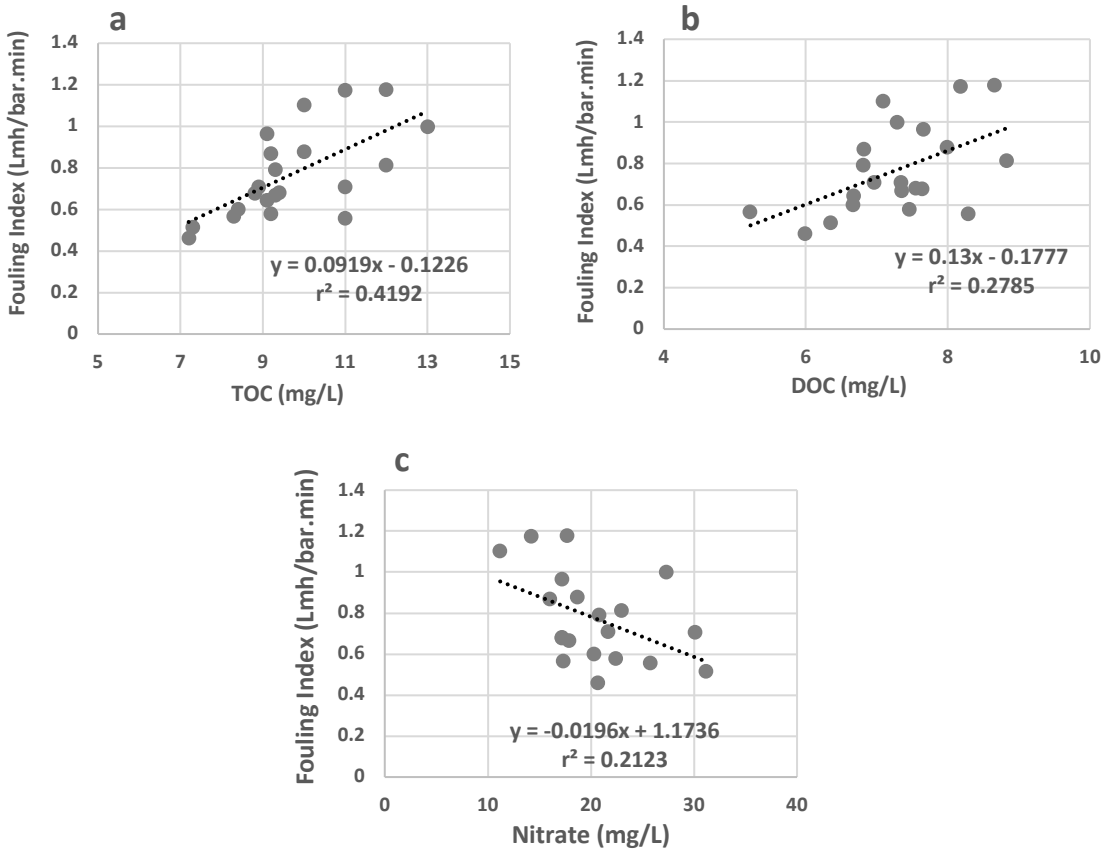


**Figure 13-Relationship between fouling index and a) TOC, b) DOC, c) nitrate**

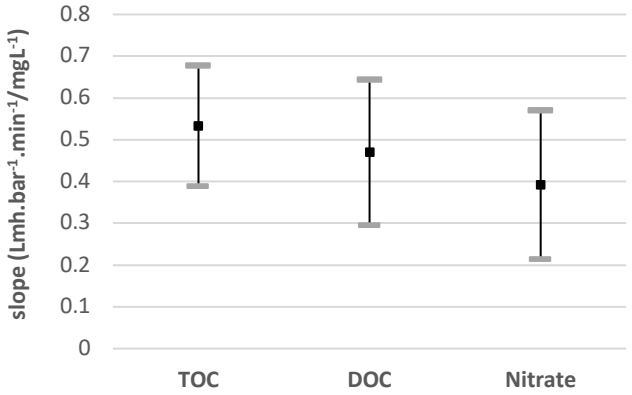


**Figure 14-Confidence intervals of regression line slope coefficients**

As can be seen in Figure 14, TOC had the highest mean slope and narrowest confidence interval. However, since the 95% confidence intervals of all variables overlapped by more than 50%, it was

concluded that the slopes were not statistically significantly different from each other (Cumming, 2009). The results indicate that the relationships between changes in TOC, DOC and nitrate concentrations in feedwater and changes in membrane fouling could not be differentiated.

It was noted that the lack of dependence of fouling on most inorganic ions observed in this study was inconsistent with those of Saravia et al., (2006) where ionic strength and calcium concentration were observed to impact permeability in MBR. In the current study, the dependence of fouling index on calcium concentration was found to be statistically insignificant with an r-squared value of 0.0958 and P-value of 0.17. The regression models used to describe all other cations and anions were also found to be insignificant with r-squared values <0.15 and P >0.05. The discrepancies in results may be due to the different types of water used in both studies. Saravia et al., (2006) used surface water from lake Hohloch, Germany, for the study with a pH of 4.5, which is acidic compared to the wastewater used in this study with an average pH of 6.8.

Abu-Obaid (2018) hypothesized that water temperature and flow affected the generation of foulants in the upstream activated sludge process. Hence, the TOC, DOC, and nitrate concentrations were plotted against these variables to assess whether similar trends existed (Figures 15-17). As can be seen in Figure 15, the r-squared values for the relationships between TOC, temperature, and flow were 0.0804 (P = 0.21) and 0.001 (P = 0.91) respectively. The r-squared values for the relationship between DOC, temperature, and flow were 0.0333 (P = 0.43) and 0.047 respectively (P = 0.34) (Figure 16). However, and as can be seen in Figure 17, nitrate displayed a positive correlation to temperature with an $r^2$= 0.5917 (P = 0.00033), and a negative correlation to flow with an $r^2$=0.691 (P = 5.62E-06). The results indicate no dependence of TOC and DOC on operating conditions (temperature/flow), but a dependence of nitrate on the same operating conditions.

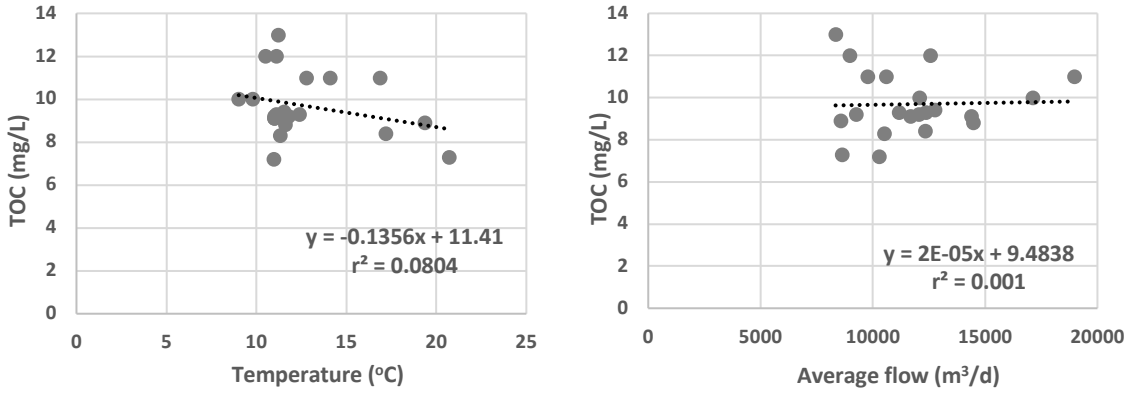


**Figure 15-Relationship between TOC, temperature (left) and average flow (right)**

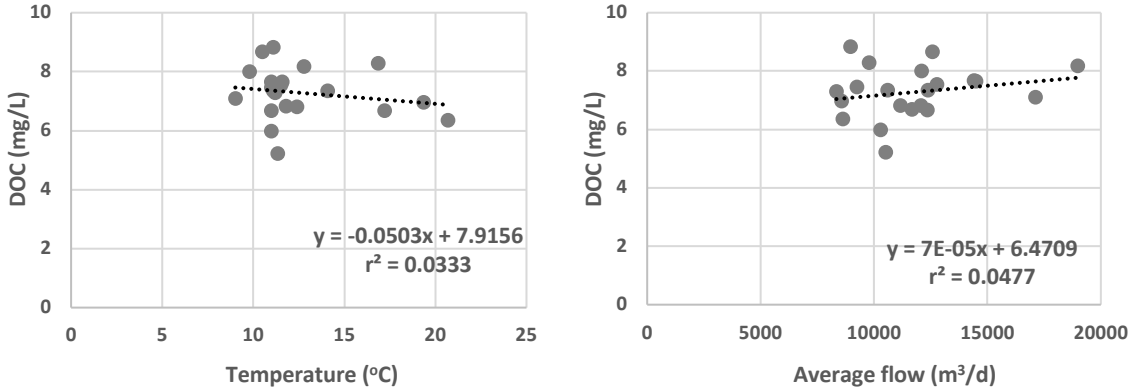


**Figure 16-Relationship between DOC, temperature (left) and average flow (right)**

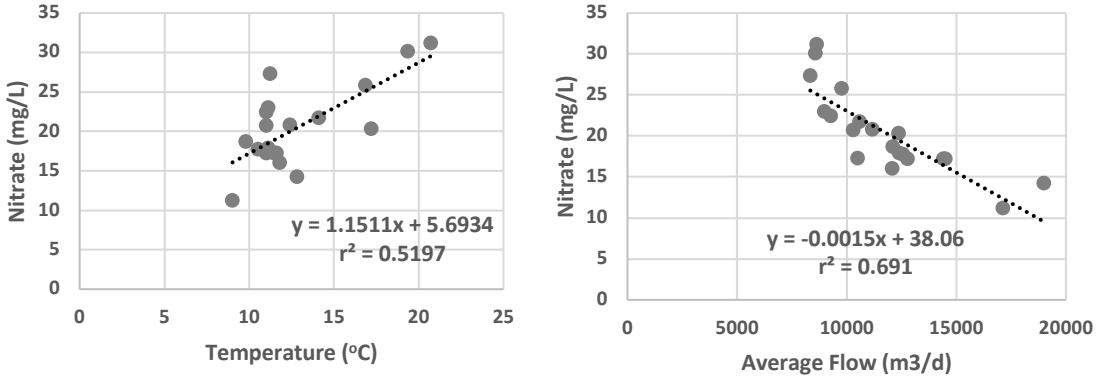


**Figure 17-Relationship between nitrate, temperature (left) and average flow (right)**

The negative correlation between the fouling index and nitrate concentration was attributed to the correlation between wastewater flows and fouling index. FI values positively correlated to wastewater flows with an increase in FI as average flow increased ($r^2$=0.3414, P=0.007). Nitrate is a product in wastewater treatment and its concentration depends on the concentration of TKN in the raw wastewater. During high flow events, TKN concentrations in the raw wastewater were observed to decrease as a result of dilution, leading to a decrease in concentration of nitrate produced in the treatment process. Hence, the correlation that was observed between FI and nitrate concentrations was due to the common impact of flow on both of these responses.

Although the changes in nitrate concentrations correlated with fouling index and flow, there was an inconsistency in the correlations between fouling, TOC/DOC concentrations and flow/temperature. To be specific, while there was no substantial dependence of TOC/DOC on flow/temperature, fouling was observed to be correlated to both flow/temperature (Figure 18) and DOC/TOC (Figure 13). It was hypothesized that this inconsistency arose from changes in the composition of the TOC/DOC with flow/temperature. Hence, to gain further insight, the five organic fractions of DOC from the LC-OCD analysis were analyzed in more detail.

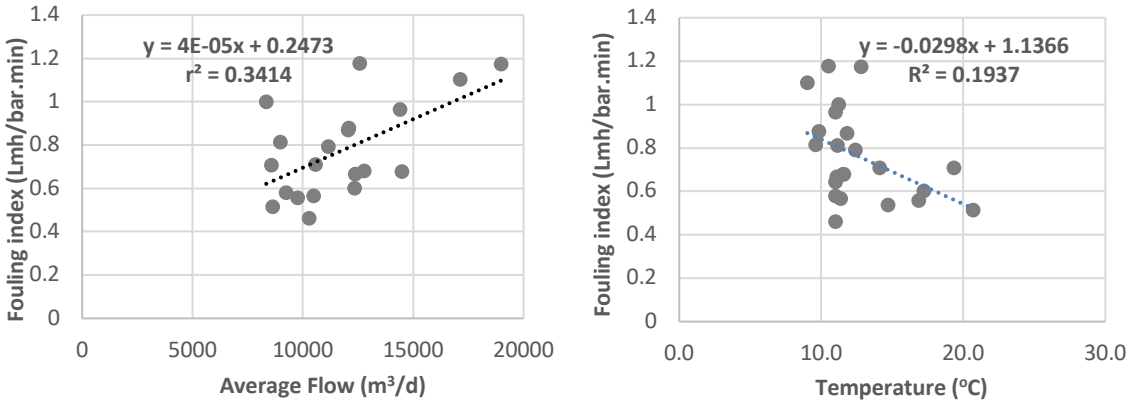


**Figure 18-Fouling index values versus wastewater flow (left), and temperature (right)**

### 4.3.2 Impact of DOM Fractions on Fouling

As seen in the previous section, there was a correlation between fouling index, DOC and TOC concentrations. In general, this was consistent with prior studies that have indicated that the

membrane feed composition especially soluble EPS is a significant contributor to fouling phenomenon (Le-Clech et al., 2008). There was however an inconsistency in the correlations between fouling, TOC/DOC and flow/temperature. Hence, to gain further insight into the fouling phenomena the fouling index was plotted versus the concentrations of the five organic fractions of DOC from the LC-OCD analysis (Figure 19) and linear regression analyses were performed. As can be seen from Figure 19, the only organic fraction that was substantially correlated with fouling index was the biopolymer fraction with an $r^2$ values of 0.57 (P = 0.000029). The relationships between FI and humic substances, building blocks, LMW acids and LMW neutrals had $r^2$ values of 0.0337 (P = 0.41), 0.0226 (P = 0.50), 0.0015 (P = 0.86), and 0.00003 (P = 0.69), respectively, and hence were not significant. It was therefore concluded that changes in fouling of tertiary membranes with seasonal variations in operational conditions likely resulted from alterations in the composition of the organics in membrane feed.

The DOC fraction results of the current study were generally consistent with prior studies of fouling in MBRs (Al-Halbouni et al.,2008; Rosenberger et al., 2006; Van der Brink et al., 2011; Sun et al., 2014; Ma et al. 2013). On the basis of these prior studies it was anticipated that biopolymers would have the highest influence on membrane fouling as UF membranes have been previously found to be fouled by substances in size range of 10 to 100 nm (Laabs et al., 2006). The results were however, inconsistent with those of Lyko et al., (2008) that suggested that carbohydrate and protein concentrations were not good indicators of sludge filterability in full-scale MBRs. However, Lyko et al. (2008) indicated that their observations could have resulted from the use of an inappropriate parameter to quantify fouling or the confounding effects of other operating parameters that prevented the establishment of correlations.

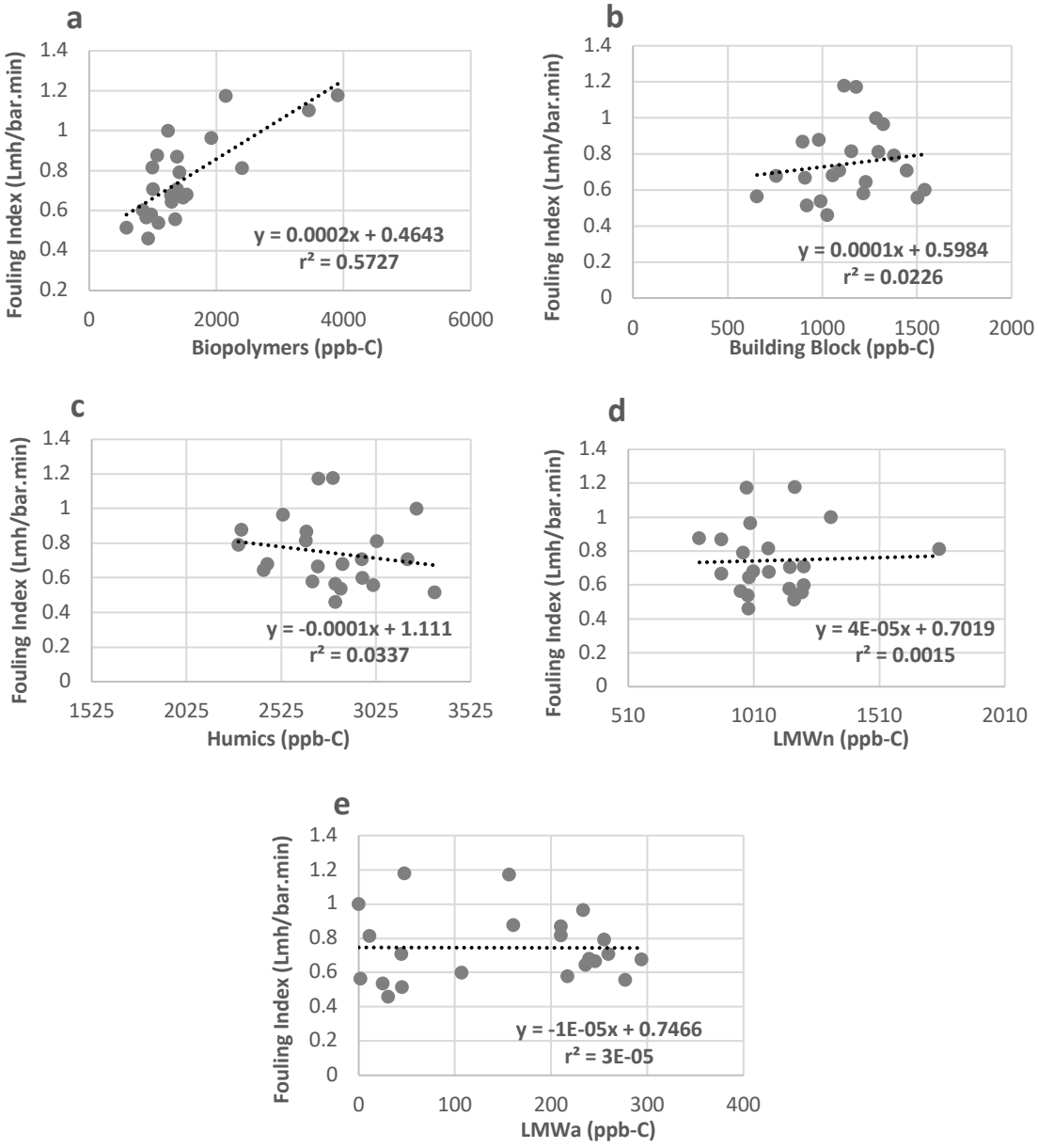


**Figure 19-Relationship between fouling index and a) biopolymers b) building blocks c) humics d) LMWn and e)LMWa**

Lyko et al. (2008) reported that significant variations in wastewater flow resulted in deviations to the food to microorganism ratio (F/M) which Kimura et al. (2005) had found to alter the nature of foulants in MBRs. Hence, it was hypothesized that dynamic changes in the wastewater flow at Keswick may have impacted the F/M which subsequently modified the foulant generation. In the

current study a strong relationship between biopolymers and fouling of the UF membranes was observed. Hence, the biopolymer concentrations were plotted against water temperature and wastewater flow to investigate whether these factors lead to the changes in biopolymer concentrations. Evenblij and Graaf (2004) found that a dilution of substrate concentration for one day did not result in changes to EPS concentrations. Hence, in this study the relationship between average flow and biopolymer concentrations was investigated for a range of flow averaging periods (1, 3, 5, 7, 9, 12 days). Correlations between the observed biopolymer concentrations and average flows were calculated separately for each averaging period. The highest correlation was found when the average of the wastewater flow on the biopolymer sampling day and the eight prior days was employed. The results for this case (Figure 20) showed a negative correlation between temperature and concentration of biopolymers, with a decrease in biopolymer concentration as temperature increased ($r^2$=0.2299, P=0.03). The results also show an increase in biopolymer concentration with the increase in average wastewater flow ($r^2$=0.1937, P=0.046).

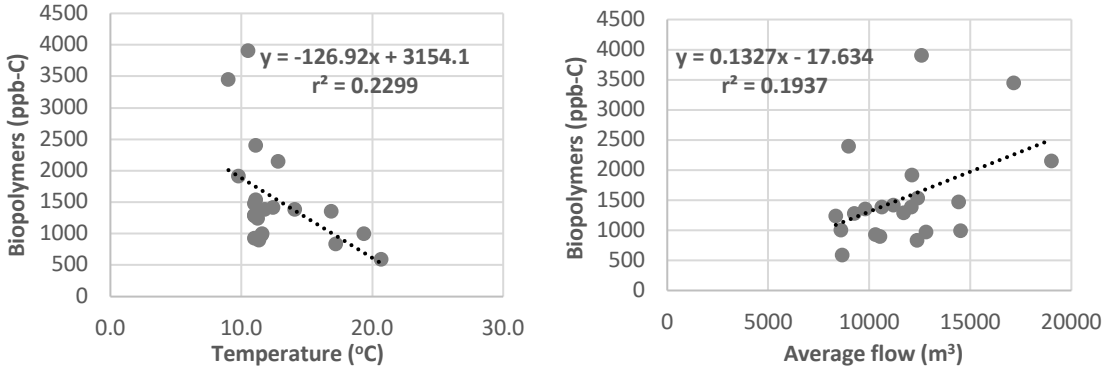


**Figure 20-Relationship between biopolymer concentration of total DOC, temperature (left) and average flow (right)**

It was previously demonstrated that fouling indexes increased with the concentrations of TOC and DOC however, there was no correlation between TOC and DOC concentrations and either temperature or flow ($r^2$< 0.08). Similarly, higher biopolymer (Bp) concentrations lead to higher values of the fouling index and appeared to be generated at lower temperature and higher flows. To investigate the hypothesis that this inconsistency arose from changes in the composition of the TOC/DOC with flow/temperature, the fraction of Bp/DOC was plotted against flow and temperature (Figure 21). As can be seen in the figure, there was a negative correlation between Bp/DOC ratio and

temperature, with a decrease in Bp/DOC as temperature increased ($r^2$=0.296, P=0.02). There was also a positive correlation between Bp/DOC ratio and flow, with an increase in Bp/DOC as flow increases ($r^2$=0.224, P=0.03). Since it was previously shown that TOC and DOC concentrations did not change with changes in temperature/flow, the correlation between Bp/DOC and temperature/flow was deemed to be responsible for the observed correlation between fouling index and TOC/DOC. Hence, it was concluded that fouling was a result of alterations in the composition of TOC/DOC with flow/temperature.

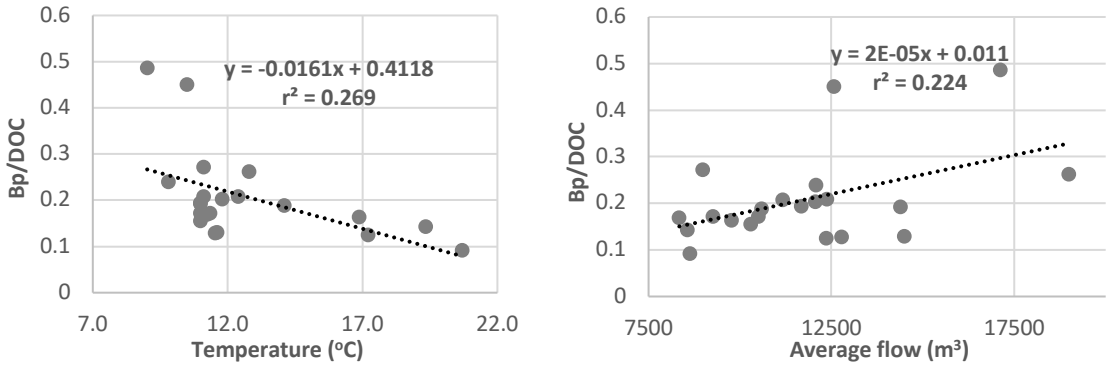


**Figure 21-Relationship between Bp/DOC, temperature (left) and average flow (right)**

### 4.3.3 Variation of Sludge Dewaterability

As mentioned previously, prior research has shown that operating an activated sludge process under cold water conditions lead to a reduction in sludge dewaterability (Lyko et al., (2007), Al-Halbouni et al., (2008), and Le-Clech et al., 2006). Lyko et al. (2007) and Al-Halbouni et al. (2008) related the deterioration of sludge dewaterability to the increase in carbohydrates and EPS concentration in the mixed liquor. Le-Clech et al. (2006) observed an increase in CST with the increase in fouling rates and soluble carbohydrates. In the current study the relationship between fouling index and CST was investigated and the results are shown in Figure 22. As can be seen in the figure, there was an evident positive linear correlation between fouling index and CST with an r-squared value of 0.6085 (P= 0.0001). In addition, the relationship between biopolymer concentration, as determined by LC-OCD that includes carbohydrates and proteins, and fouling index was investigated (Figure 22). From Figure 22, it can be seen that there was a positive linear relationship between both parameters with an r-

squared value of 0.4627 (P= 0.001). The increase in CST with biopolymer concentration was consistent with the findings of Le-Clech et al. (2006).

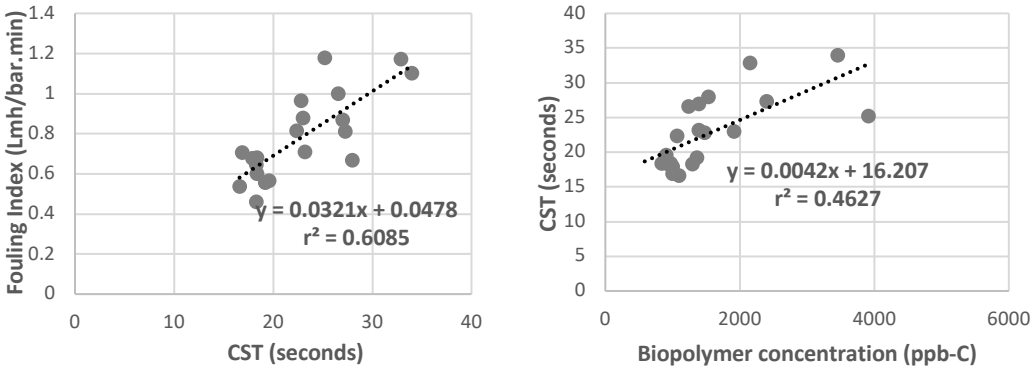


**Figure 22-Relationship between fouling index and CST (left), and CST and biopolymer concentration (right)**

To investigate whether the CST responses were affected by changes in operating conditions, CST values were plotted against temperature and flow (Figure 23). As can be seen in Figure 23, the r-squared values for the relationship between CST, temperature, and flow were 0.2148 (P=0.04) and 0.2459 (P=0.03) respectively. Hence, it was concluded that sludge dewaterability was negatively impacted (higher CST) with decreases in temperature and increases in average flow, and hence could potentially be used as indirect indicator of membrane fouling potential in tertiary membrane processes.

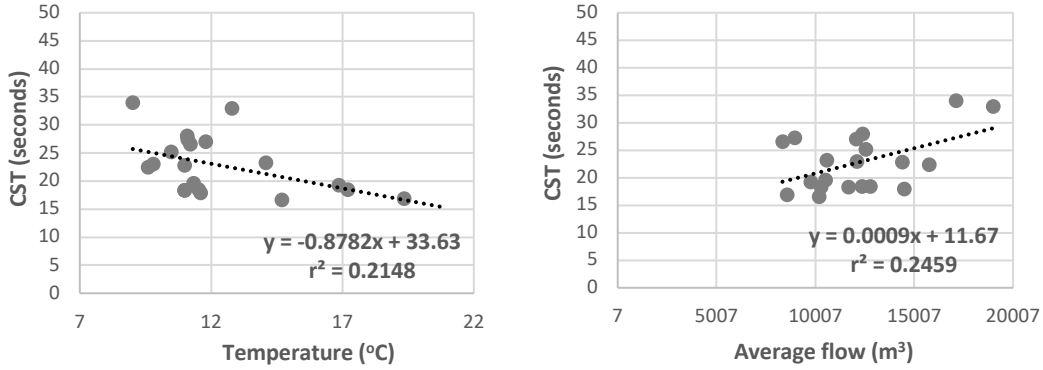


**Figure 23-Relationship between CST, temperature (left) and average flow (right)**

### 4.3.4 Investigating Source of Foulants

The observed strong correlation between biopolymer concentrations and membrane fouling suggested the importance of determining the source of foulants system. Krzeminski et al., (2011), suggested that higher level of organics at low temperatures were a result of reduced hydrolysis of foulants that were present in raw wastewater. Rosenberger et al., (2006) and Gao et al., (2013), suggested that the potential foulants, EPS, and SMP were produced by biomass as a result of biological or mechanical stress. In order to investigate the possible foulant sources in the current study, raw wastewater and membrane feed samples were analyzed using LC-OCD and the resulting biopolymer concentrations were plotted versus observed fouling index in Figure 24. As can be seen in Figure 24, the concentration of biopolymers in the membrane feed stream were consistently lower than that in raw wastewater for all samples collected on days with fouling index lower than 1 Lmh/bar.min. For days with a fouling index exceeding 1 Lmh/bar.min, the biopolymer concentrations in the membrane feed were higher than that of the raw wastewater. The difference between the biopolymer concentrations were slight when fouling index was 1 Lmh/bar.min. However, the difference in concentrations became more prominent as fouling index exceeded 1 Lmh/bar.min. The results suggest that the foulants were being generated by the biomass in the activated sludge process during the periods of higher fouling.

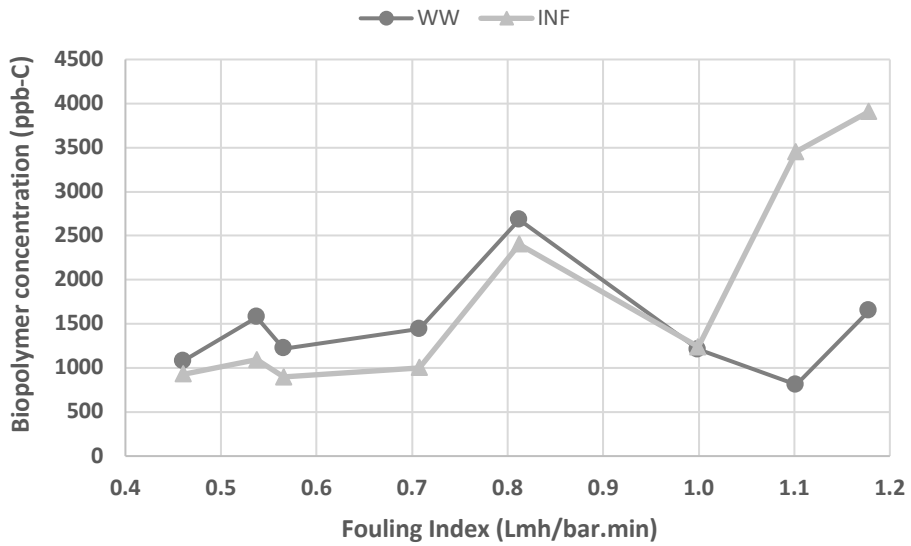


**Figure 24-Biopolymer concentrations of total DOC in raw wastewater and membrane influent streams**

## 4.4 Conclusions and Recommendations

A suite of conventional and novel water quality parameters were measured over a 17-month study period to identify which water characteristics lead to higher fouling during periods of low water temperatures and higher flows. The following conclusions were drawn from the results of this study:

1. Higher fouling indexes were found to correlate to elevated biopolymer concentrations. The increase in biopolymer concentrations corresponded to a decrease in water temperature and higher flows.
2. Fouling index was found to be correlated to TOC, DOC, and nitrate concentrations. However, no correlation was found between TOC and DOC concentrations and variation in operational conditions (temperature/flow). The results indicated that fouling of tertiary membranes due to seasonal variation in activated sludge operational conditions resulted from alterations in the composition of the organics in membrane feed, not the overall concentration of DOC.
3. Fouling in tertiary membranes was observed to correlate with the deterioration of activated sludge dewaterability, as indicated by elevated CST. This is believed to be a result of an increased concentration of biopolymers in the mixed liquor.
4. Higher CST values were found to be a result of low water temperatures and higher flows as a result of seasonal variations
5. Higher concentrations of biopolymers in the membrane feed, in comparison to raw wastewater, were observed during periods with minimum fouling index of 1 Lmh/bar.min. The results indicate that foulants are produced by biomass in the activated sludge process during periods of higher fouling.

It is recommended that a bench-scale study be conducted to investigate the effect of water temperature and flows separately on fouling of tertiary membranes. This will be necessary to gain better insight into the fouling mechanisms of membranes under various operational conditions.

# Chapter 5- Conclusions and Recommendations

## 5.1 Summary of Conclusions

The motivation for this project stemmed from the lack of literature addressing fouling of tertiary membranes under stressful operating conditions. Tertiary membranes have been reported to have high fouling rates in early spring periods which are characterized by low wastewater temperatures and elevated flows. The goal of this study was to identify critical operating conditions leading to seasonal fluctuations in fouling in these types of systems. In addition, changes in potential foulants during high fouling periods were examined to obtain an improved understanding of the foulant characteristics. The project goals were achieved through a historical review of membrane operations and an extended term characterization of feedwater quality during extreme operational conditions.

It was found that membrane fouling was similar in two parallel trains indicating that fouling was independent of train used. Increased recoveries of permeability as a result of membrane back-pulses, MCs and RCs were observed during high fouling events, and hence it was concluded that fouling was not a result of reduced efficiency of membrane cleaning under cold water conditions. The results showed a relationship between rapid membrane performance deterioration between cleans (BPs, MCs and RCs) and water temperature and flow, which was more than could be explained by changes in water viscosity with temperature. The differing fouling behaviour patterns between the two year-long observation periods suggested a more complex dependence of fouling on operating conditions, which was investigated through the characterization of foulant characteristics during high fouling events.

The examination of feedwater quality data revealed that high fouling rates correlated to an increase in TOC and DOC concentrations, and a decrease in nitrate concentrations. The analysis of LC-OCD results revealed that increase in fouling rates also correlated to higher biopolymer concentrations of total DOC. The increase in biopolymer concentrations and decrease in nitrate concentrations were correlated to the decrease in water temperature and increase in flow. However, no relationship was observed between TOC and DOC concentrations and temperature and flow. Therefore, the correlation between fouling and TOC/DOC was linked to the change in composition of organics in membrane feed during extreme operational conditions. The correlation between fouling index and nitrate was explained by the dilution of TKN in raw wastewater feed during elevated flow events. The examination of field data also revealed an increase in CST values during high fouling events. The

increase in CST values correlated to the decrease in water temperature and increase in flow. Elevated CST values, which indicate worsened sludge dewaterability, also correlated to higher biopolymer concentrations. Therefore, it was concluded that seasonal variations may result in the increased release of EPS by microorganisms. This leads to higher membrane fouling and worsened dewaterability of upstream sludge.

The characteristics of membrane feedwater were compared to raw wastewater in order to determine the potential source of foulants. It was observed that during high fouling events, the concentrations of biopolymers, which were recognized as key foulants, in secondary effluent exceeded concentrations in bioreactor influent (raw wastewater). This indicates that increased fouling and deterioration in sludge dewaterability is due to increased release of organics (EPS and SMP) by microorganisms under stressed operating conditions.

The results of this study enhance the overall understanding of patterns in fouling behaviour and foulant characteristics of tertiary membranes operating under stressed conditions. This knowledge can be employed to assist with the design of mitigation strategies to reduce costs of these types of systems. Further, an enhanced understanding of seasonal variations that lead to increased fouling, and identification of fouling indicators, can allow for the prediction of upcoming fouling events, and employment of mitigation strategies when needed.

## 5.2 Recommendations

In the current study it was not possible to delineate the contributions of the temperature and flow due to correlations between them. Hence, it is recommended that controlled testing be conducted to isolate their individual contributions and compare the relative significance of each to overall fouling.

It is also recommended that the mechanisms at which flow affects fouling be further investigated. This should be done through studying the influence of dynamic fluctuations in HRT and F/M ratio on foulant characteristics. The results suggest that the challenge seasonal variations impose on these types of systems is through the dynamic change in operating conditions. However, research is usually focused on steady-state operations. Therefore, it is important for dynamic changes in operating conditions be further studied.

# Bibliography


Abdullah, Syed Z., and Pierre R. Bérubé. 2013. "Assessing the Effects of Sodium Hypochlorite Exposure on the Characteristics of PVDF Based Membranes." *Water Research* 47 (14): 5392–99. https://doi.org/10.1016/j.watres.2013.06.018.

Ahmed, Zubair, Jinwoo Cho, Byung Ran Lim, Kyung Guen Song, and Kyu Hong Ahn. 2007. "Effects of Sludge Retention Time on Membrane Fouling and Microbial Community Structure in a Membrane Bioreactor." *Journal of Membrane Science* 287 (2): 211–18. https://doi.org/10.1016/j.memsci.2006.10.036.

Al-Halbouni, Djamila, Jacqueline Traber, Sven Lyko, Thomas Wintgens, Thomas Melin, Daniela Tacke, Andreas Janot, Wolfgang Dott, and Juliane Hollender. 2008. "Correlation of EPS Content in Activated Sludge at Different Sludge Retention Times with Membrane Fouling Phenomena." *Water Research* 42 (6–7): 1475–88. https://doi.org/10.1016/j.watres.2007.10.026.

APHA Standard Methods for the Examination of Water and Wastewater, 22nd ed., American Public Health Association, Washington, DC, 2017.

Arévalo, Juan, Gloria Garralón, Fidel Plaza, Begoña Moreno, Jorge Pérez, and Miguel Ángel Gómez. 2009. "Wastewater Reuse after Treatment by Tertiary Ultrafiltration and a Membrane Bioreactor (MBR): A Comparative Study." *Desalination* 243 (1–3). Elsevier B.V.: 32–41. https://doi.org/10.1016/j.desal.2008.04.013.

Chen, G.W., W.W. Lin, and D.J. Lee. 1996. "Capillary Suction Time CST as a Measure of Sludge Dewaterability." Great Britain: Elsevier Ltd.

Citulski, Joel a, Khosrow Farahbakhsh, and Fraser C Kent. 2009. "Effects of Total Suspended Solids Loading on Short-Term Fouling in the Treatment of Secondary Effluent by an Immersed Ultrafiltration Pilot System." *Water Environment Research* 81 (12): 2427–36. https://doi.org/10.2175/106143009X426022.

Croft, Jamie. 2012. "Natural Organic Matter Characterization of Different Source and Treated Waters ; Implications for Membrane Fouling Control" (Unpublished master's thesis). University of Waterloo, Waterloo, Ontario, Canada.

Cumming, Geoff. 2009. "Growth Rates in Epidemic Models: Application to a Model for HIV/AIDS Progression." *Statistics in Medicine* 28 (July 2006): 221–39. https://doi.org/10.1002/sim.

Díaz, Oliver, Luisa Vera, Enrique González, Elisa García, and Juan Rodríguez-Sevilla. 2016. "Effect of Sludge Characteristics on Membrane Fouling during Start-up of a Tertiary Submerged Membrane Bioreactor." *Environmental Science and Pollution Research* 23 (9): 8951–62. https://doi.org/10.1007/s11356-016-6138-y.

Drews, Anja. 2010. "Membrane Fouling in Membrane Bioreactors-Characterisation, Contradictions, Cause and Cures." *Journal of Membrane Science* 363 (1–2). Elsevier B.V.: 1–28. https://doi.org/10.1016/j.memsci.2010.06.046.

Evenblij, H., and J. H J M van der Graaf. 2004. “Occurrence of EPS in Activated Sludge from a Membrane Bioreactor Treating Municipal Wastewater.” *Water Science and Technology* 50 (12): 293–300.

Gao, Da Wen, Zhi Dan Wen, Bao Li, and Hong Liang. 2013. “Membrane Fouling Related to Microbial Community and Extracellular Polymeric Substances at Different Temperatures.” *Bioresource Technology* 143. Elsevier Ltd: 172–77. https://doi.org/10.1016/j.biortech.2013.05.127.

Huber, Stefan A., and Fritz H. Frimmel. 1991. “Flow Injection Analysis of Organic and Inorganic Carbon in the Low-Ppb Range.” *Analytical Chemistry* 63 (19): 2122–30. https://doi.org/10.1021/ac00019a011.

Jones, Thomas. 1972. “Multiple Regression with Correlated Independent Variables 1.” *Mathematical Geology* 4 (3): 203–18.

Kent, Fraser C., Joel Citulski, and Khosrow Farahbakhsh. 2011. “Water Reclamation Using Membranes: Permeate Water Quality Comparison of MBR and Tertiary Membrane Filtration.” *Desalination* 274 (1–3). Elsevier B.V.: 237–45. https://doi.org/10.1016/j.desal.2011.02.019.

Kimura, Katsuki, Nobuhiro Yamato, Hiroshi Yamamura, and Yoshimasa Watanabe. 2005. “Membrane Fouling in Pilot-Scale Membrane Bioreactors (MBRs) Treating Municipal Wastewater.” *Environmental Science and Technology* 39 (16): 6293–99. https://doi.org/10.1021/es0502425.

Krzeminski, P., A. Iglesias-Obelleiro, G. Madebo, J. M. Garrido, J. H.J.M. van der Graaf, and J. B. van Lier. 2012. “Impact of Temperature on Raw Wastewater Composition and Activated Sludge Filterability in Full-Scale MBR Systems for Municipal Sewage Treatment.” *Journal of Membrane Science* 423–424. Elsevier: 348–61. https://doi.org/10.1016/j.memsci.2012.08.032.

Laabs, Claudia N., Gary L. Amy, and Martin Jekel. 2006. “Understanding the Size and Character of Fouling-Causing Substances from Effluent Organic Matter (EfOM) in Low-Pressure Membrane Filtration.” *Environmental Science and Technology* 40 (14): 4495–99. https://doi.org/10.1021/es060070r.

Lankes, Ulrich, Margit B. Müller, Matthias Weber, and Fritz H. Frimmel. 2009. “Reconsidering the Quantitative Analysis of Organic Carbon Concentrations in Size Exclusion Chromatography.” *Water Research* 43 (4): 915–24. https://doi.org/10.1016/j.watres.2008.11.025.

Le-Clech, Pierre, Vicki Chen, and Tony A.G. Fane. 2006. “Fouling in Membrane Bioreactors Used in Wastewater Treatment.” *Journal of Membrane Science* 284 (1–2): 17–53. https://doi.org/10.1016/j.memsci.2006.08.019.

Liang, Shuang, Cui Liu, and Lianfa Song. 2007. “Soluble Microbial Products in Membrane Bioreactor Operation: Behaviors, Characteristics, and Fouling Potential.” *Water Research* 41 (1): 95–101. https://doi.org/10.1016/j.watres.2006.10.008.

Lyko, Sven, Thomas Wintgens, Djamila Al-Halbouni, Sven Baumgarten, Daniela Tacke, Kinga Drensla, Andreas Janot, Wolfgang Dott, Johannes Pinnekamp, and Thomas Melin. 2008. "Long-Term Monitoring of a Full-Scale Municipal Membrane Bioreactor-Characterisation of Foulants and Operational Performance." *Journal of Membrane Science* 317 (1–2): 78–87. https://doi.org/10.1016/j.memsci.2007.07.008.

Ma, Zhun, Xianghua Wen, Fang Zhao, Yu Xia, Xia Huang, David Waite, and Jing Guan. 2013. "Effect of Temperature Variation on Membrane Fouling and Microbial Community Structure in Membrane Bioreactor." *Bioresource Technology* 133. Elsevier Ltd: 462–68. https://doi.org/10.1016/j.biortech.2013.01.023.

Martín-Pascual, J., J. C. Leyva-Díaz, C. López-López, M. M. Muñio, E. Hontoria, and J. M. Poyatos. 2015. "Effects of Temperature on the Permeability and Critical Flux of the Membrane in a Moving Bed Membrane Bioreactor." *Desalination and Water Treatment* 53 (13). Taylor & Francis: 3439–48. https://doi.org/10.1080/19443994.2013.873879.

Massé, Anthony, Mathieu Spérandio, and Corinne Cabassud. 2006. "Comparison of Sludge Characteristics and Performance of a Submerged Membrane Bioreactor and an Activated Sludge Process at High Solids Retention Time." *Water Research* 40 (12): 2405–15. https://doi.org/10.1016/j.watres.2006.04.015.

Meng, Fangang, So Ryong Chae, Anja Drews, Matthias Kraume, Hang Sik Shin, and Fenglin Yang. 2009. "Recent Advances in Membrane Bioreactors (MBRs): Membrane Fouling and Membrane Material." *Water Research* 43 (6). Elsevier Ltd: 1489–1512. https://doi.org/10.1016/j.watres.2008.12.044.

Miyoshi, Taro, Tomoo Tsuyuhara, Rie Ogyu, Katsuki Kimura, and Yoshimasa Watanabe. 2009. "Seasonal Variation in Membrane Fouling in Membrane Bioreactors (MBRs) Treating Municipal Wastewater." *Water Research* 43 (20). Elsevier Ltd: 5109–18. https://doi.org/10.1016/j.watres.2009.08.035.

Philippe, Nicolas, Anne Emmanuelle Stricker, Yvan Racault, Alain Husson, Mathieu Sperandio, and Peter Vanrolleghem. 2013. "Modelling the Long-Term Evolution of Permeability in a Full-Scale MBR: Statistical Approaches." *Desalination* 325. Elsevier B.V.: 7–15. https://doi.org/10.1016/j.desal.2013.04.027.

Rosenberger, S., C. Laabs, B. Lesjean, R. Gnirss, G. Amy, M. Jekel, and J. C. Schrotter. 2006. "Impact of Colloidal and Soluble Organic Material on Membrane Performance in Membrane Bioreactors for Municipal Wastewater Treatment." *Water Research* 40 (4): 710–20. https://doi.org/10.1016/j.watres.2005.11.028.

Saravia, Florencia, Christian Zwiener, and Fritz H. Frimmel. 2006. "Interactions between Membrane Surface, Dissolved Organic Substances and Ions in Submerged Membrane Filtration." *Desalination* 192 (1–3): 280–87. https://doi.org/10.1016/j.desal.2005.07.039.

Sun, Jianyu, Kang Xiao, Yinghui Mo, Peng Liang, Yuexiao Shen, Ningwei Zhu, and Xia Huang. 2014. "Seasonal Characteristics of Supernatant Organics and Its Effect on Membrane Fouling in a Full-Scale Membrane Bioreactor." *Journal of Membrane Science* 453. Elsevier: 168–74.

https://doi.org/10.1016/j.memsci.2013.11.003.

Sweity, Amer, Wang Ying, Mohammed S. Ali-Shtayeh, Fei Yang, Amos Bick, Gideon Oron, and Moshe Herzberg. 2011. "Relation between EPS Adherence, Viscoelastic Properties, and MBR Operation: Biofouling Study with QCM-D." *Water Research* 45 (19). Elsevier Ltd: 6430–40. https://doi.org/10.1016/j.watres.2011.09.038.

Torà-Grau, M., J. L. Soler-Cabezas, M. C. Vincent-Vela, J. A. Mendoza-Roca, and F. J. Martínez-Francisco. 2015. "Ultrafiltration Fouling Trend Simulation of a Municipal Wastewater Treatment Plant Effluent with Model Wastewater." *Desalination and Water Treatment* 56 (13): 3438–46. https://doi.org/10.1080/19443994.2014.999714.

van den Brink, Paula, On Anong Satpradit, André van Bentem, Arie Zwijnenburg, Hardy Temmink, and Mark van Loosdrecht. 2011. "Effect of Temperature Shocks on Membrane Fouling in Membrane Bioreactors." *Water Research* 45 (15): 4491–4500. https://doi.org/10.1016/j.watres.2011.05.046.

Wang, Zhiwei, Zhichao Wu, and Shujuan Tang. 2010. "Impact of Temperature Seasonal Change on Sludge Characteristics and Membrane Fouling in a Submerged Membrane Bioreactor." *Separation Science and Technology* 45 (7): 920–27. https://doi.org/10.1080/01496391003656974.

# Appendix A
# Supplementary Material

The r-squared, and P-values of the relationship between fouling index and conventional water quality parameters measured in membrane influent arranged in descending order

| Parameter | $r^2$ | P-value |
|---|---|---|
| TOC | 0.4192 (0.647) | 0.0015 <0.05 |
| DOC | 0.2785 (0.528) | 0.014<0.05 |
| Nitrate | 0.2123 (0.461) | 0.04<0.05 |
| DON | 0.174 (0.417) | 0.08>0.05 |
| Conductivity | 0.1713 (0.414) | 0.06>0.05 |
| COD | 0.1704 (0.413) | 0.07>0.05 |
| $cBOD_5$ | 0.1676 (0.409) | 0.1>0.05 |
| $K^+$ | 0.1392 (0.373) | 0.17>0.05 |
| $Cl^-$ | 0.1222 (0.35) | 0.12>0.05 |
| TKN | 0.1191 (0.345) | 0.15>0.05 |
| Turbidity | 0.1056 (0.325) | 0.13>0.05 |
| $Ca^+$ | 0.0958 (0.309) | 0.17>0.05 |
| $Na^+$ | 0.0559 (0.236) | 0.3>0.05 |
| $Mg^+$ | 0.0344 (0.185) | 0.42>0.05 |
| pH | 0.0298 (0.173) | 0.43>0.05 |
| Ammonia and $NH_4$ | 0.0215 (0.146) | 0.62> 0.05 |
| $SO_4^-$ | 0.0159 (0.126) | 0.59>0.05 |

# Appendix B
# Plant Background

The Keswick Water Pollution Control Plant was initially constructed in 1984 and in 2010 underwent major expansion to increase its design capacity from 12,070 $m^3$/d to 18,000 $m^3$/d. During the expansion, the plant's dual media tertiary filters were replaced with tertiary ultrafiltration membranes and the chlorine disinfection system was replaced with UV disinfection. Preliminary treatment system at the plant consists of a collection chamber followed by screens and a grit removal system. Preliminary treatment is followed by secondary treatment which consists of aeration system, secondary clarification, secondary scum removal, and phosphorous removal. The tertiary treatment at Keswick consists of a flocculation tank followed by micro-screens and five ultrafiltration (UF) membrane trains. The micro-screens have one millimeter openings to remove any materials larger than one millimeter to protect ultrafiltration membranes from potential damage. Each UF membrane train consists of bundles of ZeeWeed hollow-fiber modules operating under negative pressure created within the hollow fibers by permeate pumps. The plant's general process schematic can be seen in Figure below.

The UF trains are operated at a pre-determined production flow up to a maximum Trans-Membrane Pressure (TMP), or a minimum tank level. Treated water is periodically used to back-pulse (BP) the membranes to maintain stable TMP in the ultrafiltration trains. During backwash, the membranes are aerated using blowers that supply air to the membrane tanks near the bottom of the membranes to scour the outside of the membrane fibers. The membranes are also cleaned using maintenance cleans (MC) and recovery cleans (RC) to restore permeability. During MCs the membranes are soaked in sodium hypochlorite solution for 15 minutes to remove organic contaminants. For RCs, the membranes are soaked in either sodium hypochlorite or citric acid, or back to back, based on which cleaning option the operator selects, for 5 hours. Citric acid is used to remove scale and sodium hypochlorite is used for removing organic contaminants. Depending on plant demand, an ultrafiltration train proceeds to production and then back-pulse mode. This will continue until the permeate flow demand decreases, placing the train on standby. A train goes into MC or RC modes according to a set schedule, or when the membrane TMP is approaching its maximum value.

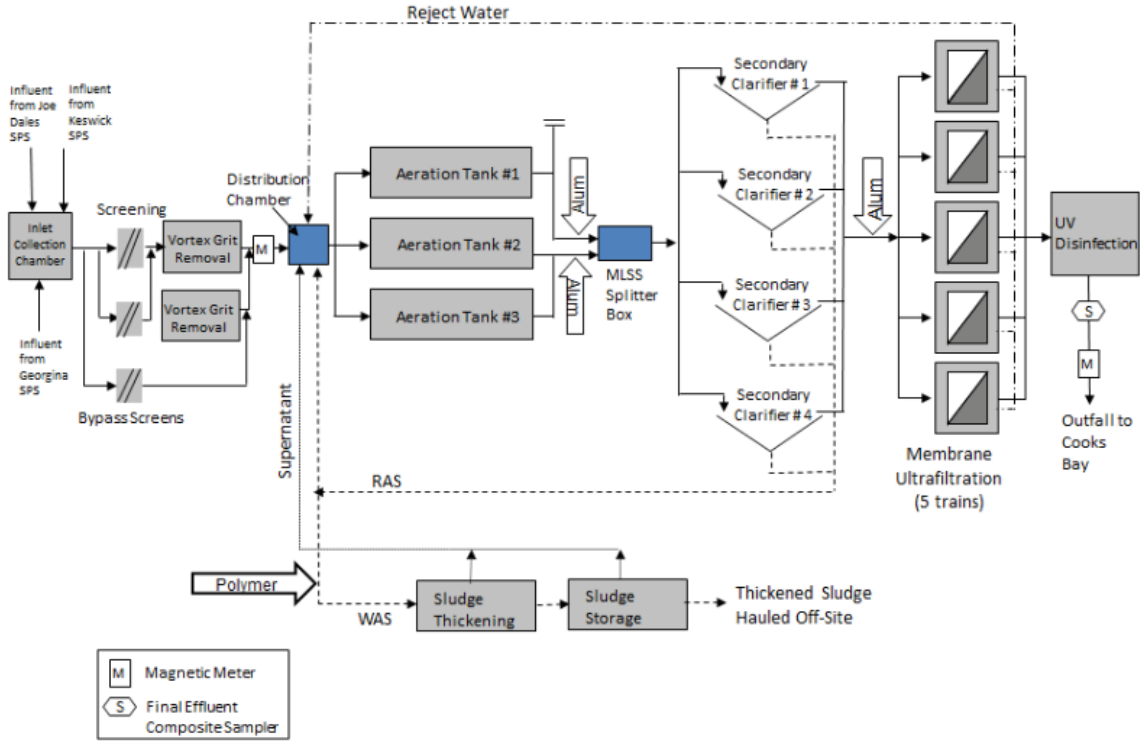


**Figure B1-General process schematic of the Keswick WPCP**

# Appendix C
# MATLAB Codes

**Code 1- Delta TCP**

**Description:**

This code calculates the difference in TCP within one cycle using the following equation:

$$\Delta TCP = P(A_N) - P(B_{N+1})$$

Where: $P(A_N)$*: TCP after back-pulse (Lmh/bar)*

$P(B_{N+1})$*: TCP before next back-pulse (Lmh/bar)*

**Input file:**

Input information should be available in a spreadsheet titled, `'UF4_RawData_2018.xlsx'`. The spreadsheet should contain the date and time of each BP, TCP during, after, and before BP, MC type, and RC type. Multiple input files should be used, one for each train and year. Figure C1 displays an example of input file.

| | A | B | C | D | E | F |
|---|---|---|---|---|---|---|
| 1 | Timestamp | UF 4-TCPermeability DuringBP | UF 4-TCPermeability AfterBP | UF 4-TCPermeability BeforeBP | UF 4-Maintenance CleanType | UF 4-Recovery CleanType |
| 2 | 01/01/2018 01:53:37 | 143.0939319 | 134.5989115 | 113.6709875 | 0 | 0 |
| 3 | 01/01/2018 06:35:07 | 142.7652958 | 134.1221753 | 103.2540031 | | |
| 4 | 01/01/2018 10:53:56 | 142.5369542 | 135.2755441 | 100.4607468 | | |
| 5 | 01/01/2018 13:55:08 | | | | 4 | |
| 6 | 01/01/2018 16:30:27 | 141.2465094 | 139.4678322 | 103.8424404 | | |
| 7 | 01/01/2018 21:35:45 | 148.5625602 | 143.9172275 | 126.6245227 | | |
| 8 | 01/02/2018 04:46:03 | 144.277574 | 139.0049691 | 107.115929 | | |
| 9 | 01/02/2018 10:23:57 | 144.4640208 | 132.4151251 | 112.7006937 | | |
| 10 | 01/02/2018 13:13:23 | 143.2394355 | 136.4322908 | 118.4553702 | | |
| 11 | 01/02/2018 19:30:02 | 142.0190682 | 136.4468085 | 100.7469344 | | |
| 12 | 01/02/2018 22:42:36 | | | | | 1 |
| 13 | 01/03/2018 14:57:26 | 168.6102576 | 168.327052 | 132.7560857 | | |
| 14 | 01/03/2018 19:04:53 | 164.8302639 | 162.6811856 | 131.8876005 | | |
| 15 | 01/03/2018 22:25:59 | 162.3235546 | 159.8764551 | 124.1056223 | | |

**Figure C1- Layout of input file**

**Output information:**

This code will output two arrays: `dates` and `deltaBP`. The `dates` array contains the date and time of the BP that starts the cycle. The `deltaBP` array contains the change in TCP between the start and end of the cycle.

```
clc, clear all, close all


% Raw Data recall
AA=readtable('UF4_RawData_2018.xlsx');
[n,m]=size(AA);

B = xlsread('UF4_RawData_2018.xlsx',1, 'B:B'); % TCP during BP
D = xlsread('UF4_RawData_2018.xlsx',1, 'C:C'); % TCP after BP
C = xlsread('UF4_RawData_2018.xlsx',1, 'D:D'); % TCP before BP
E = xlsread('UF4_RawData_2018.xlsx',1, 'E:E'); % MC type
F = xlsread('UF4_RawData_2018.xlsx',1, 'F:F'); % RC type
flag=0;
% creating empty arrays
deltaBP=[];
dates=[];

for i=2:(n-1)
    if (flag==0)
        if (E(i)~=4 || F(i)~=1 || F(i)~=2)
            BP= D(i-1)-C(i);
            d= AA.Timestamp(i-1);
            deltaBP =[deltaBP, BP];
            dates=[dates, d];
        end
    end

        if (flag==0) && ((E(i)==4 || F(i)==1 ||F(i)==2) && (E(i+1)~=4 ||
F(i+1)~=1|| F(i+1)~=2))
            BP=D(i-1)-C(i+1);
            d=AA.Timestamp(i);
            deltaBP =[deltaBP, BP];
            dates=[dates, d];
            flag=1;

        end
      if (flag==1) && (E(i+1)==4 || F(i+1)==1 || F(i+1)==2)
            BP=D(i-1)-C(i+2);
            d=AA.Timestamp(i);
            deltaBP =[deltaBP, BP];
            dates=[dates, d];
            flag=2;
       end

        if ((flag==1 || flag==2)&& (E(i-1)==4 || F(i-1)==1 || F(i-1)==2))
            if (E(i)~=4 && F(i)~=1)
                flag = 0;
                continue;
            end
        end
end
dates= datetime(dates);
dates'
deltaBP = deltaBP'
```

**Code 2- Delta t**

**Description:**

This code calculates the length of permeation within a cycle. This is done through counting the number of permeation codes (13XX) between two BPs (34XX).

**Input file:**

Input information should be available in spreadsheet titled, `'UF1-2018.xlsx'`. The spreadsheet should contain the date, time, and train status code recorded every minute. Multiple input files should be used, one for each train and year. Figure C2 displays an example of input file.

| | A | B |
|---|---|---|
| 1 | **Timestamp** | **code** |
| 2 | 2018-Jan-01 00:00:00 | 504 |
| 3 | 2018-Jan-01 00:01:00 | 504 |
| 4 | 2018-Jan-01 00:02:00 | 504 |
| 5 | 2018-Jan-01 00:03:00 | 504 |
| 6 | 2018-Jan-01 00:04:00 | 504 |
| 7 | 2018-Jan-01 00:05:00 | 504 |
| 8 | 2018-Jan-01 00:06:00 | 504 |
| 9 | 2018-Jan-01 00:07:00 | 504 |
| 10 | 2018-Jan-01 00:08:00 | 504 |
| 11 | 2018-Jan-01 00:09:00 | 504 |
| 12 | 2018-Jan-01 00:10:00 | 504 |
| 13 | 2018-Jan-01 00:11:00 | 504 |
| 14 | 2018-Jan-01 00:12:00 | 504 |
| 15 | 2018-Jan-01 00:13:00 | 504 |
| 16 | 2018-Jan-01 00:14:00 | 504 |
| 17 | 2018-Jan-01 00:15:00 | 504 |
| 18 | 2018-Jan-01 00:16:00 | 504 |
| 19 | 2018-Jan-01 00:17:00 | 504 |
| 20 | 2018-Jan-01 00:18:00 | 504 |

**Figure C2- Train status codes recorded every minute**

**Output information:**

This code will output two arrays: `dates` and `CC`. The `dates` array contains the date and time of the first permeation code (13XX) recorded after a clean is completed (BP,MC, or RC). The `CC` array contains the number of minutes of permeation between two cleans (BP, MC, or RC).

```
clc, clear all, close all
format short
% importing the data from excel
AA = readtable('UF1-2018.xlsx');
[n,m]=size(AA);
B=xlsread('UF1-2018.xlsx',1, 'B:B');
d1=AA.Timestamp;
Date1= datetime(d1,'InputFormat','yyyy-MM-dd HH:mm:ss');

%initalize the count-
count=0;
%this flag variable triggers the count
flag = 0;
%an array to store the results
cycle = [];
dates = [];


for i=1:(n)
     %this flag checks if the count is on and the device reading becomes
     %3405
     if ((count > 0) && (flag == 1) && (B(i)>=3401))
         %date2 = AA.Timestamp(i+1);
         cycle = [cycle, count];
         %dates = [dates, date2];
         flag = 0;
     end
     %This loops triggers the counter once and set the flag
     if (B(i)>=3401)
         count= 0;
         flag = 1;
     end


     %This loops only works only if the flag is on, and the counter
     %increments if the value is 1302 or 1303
     if((flag == 1) && (B(i) == 1302 || B(i) == 1303 || B(i)==1301))
         count = count + 1;
     if (count==1)
         date2 = Date1(i);
         dates = [dates, date2];
     end
     end
end

% display of results

CC=[cycle]';
dates=dates'
```

**Code 3- Fouling index (FI)**

**Description:**

This code uses the delta TCP calculated using Code 1, and the length of permeation (delta t) calculated using Code 2, to determine the fouling index per cycle using the following equation:

$$FI = \frac{\Delta TCP}{\Delta t}$$

Where: $\Delta TCP$*: Difference in TCP between the beginning and end of a cycle (Lmh/bar)*

$\Delta t$*: Length of permeation between consecutive BP (minute)*

**Input file:**

This code requires two input files:

1. Spreadsheet titled, `'TCP.xlsx'`: contains the output of Code 1 (See Figure C3)
2. Spreadsheet titled, `'length.xlsx'`: contains the output of Code 2 (See Figure C4)

| | A | B |
|---|---|---|
| 1 | Date | BPFouling |
| 2 | 01-Jan-2018 01:53:37 | 31.3449 |
| 3 | 01-Jan-2018 06:35:07 | 33.6614 |
| 4 | 01-Jan-2018 10:53:56 | NaN |
| 5 | 01-Jan-2018 13:55:08 | 31.4331 |
| 6 | 01-Jan-2018 16:30:27 | 12.8433 |
| 7 | 01-Jan-2018 21:35:45 | 36.8013 |
| 8 | 02-Jan-2018 04:46:03 | 26.3043 |
| 9 | 02-Jan-2018 10:23:57 | 13.9598 |
| 10 | 02-Jan-2018 13:13:23 | 35.6854 |
| 11 | 02-Jan-2018 19:30:02 | NaN |
| 12 | 02-Jan-2018 22:42:36 | 3.6907 |
| 13 | 03-Jan-2018 14:57:26 | 36.4395 |
| 14 | 03-Jan-2018 19:04:53 | 38.5756 |

**Figure C3- Delta TCP outputs of Code 1**

| | A | B |
|---|---|---|
| 1 | Date | Length |
| 2 | 01-Jan-2018 06:09:00.000 | 100 |
| 3 | 01-Jan-2018 10:28:00.000 | 109 |
| 4 | 01-Jan-2018 16:04:00.000 | 69 |
| 5 | 01-Jan-2018 21:10:00.000 | 96 |
| 6 | 02-Jan-2018 04:20:00.000 | 108 |
| 7 | 02-Jan-2018 09:58:00.000 | 65 |
| 8 | 02-Jan-2018 12:47:00.000 | 77 |
| 9 | 02-Jan-2018 19:04:00.000 | 6 |
| 10 | 03-Jan-2018 07:21:00.000 | 115 |
| 11 | 03-Jan-2018 14:31:00.000 | 109 |
| 12 | 03-Jan-2018 18:39:00.000 | 104 |

**Figure C4- Length of permeation output of Code 2**

**Output information:**

This code will output two arrays: `dates` and `foul`. The `dates` array contains the date and time of each cycle for which a fouling index was calculated. The `foul` array contains the fouling index calculated for each cycle.

```
clc, clear all, close all, format long

% Raw data
length= readtable ('length.xlsx');
TCPP= readtable('TCP.xlsx');
[n,mm]= size(length);
[x,y]= size (TCPP);
dateleng=length.Date;
len=length.Length;
datetcp= TCPP.Date;
TCP= TCPP.BPFouling;
dleng= datetime(dateleng,'InputFormat','dd-MMM-yyyy HH:mm:ss.sss');
dtcp= datetime(datetcp,'InputFormat','dd-MMM-yyyy HH:mm:ss');

% Length
dl= day(dleng);
ml= month(dleng);
[h,m,s]=hms(dleng);

% TCP
dt= day(dtcp);
mt= month(dtcp);
[h2,m2,s2]=hms(dtcp);

foul=[]; dates=[]; lengg=[];
%%%%%%%%%%%%%%%%%%%%%%%%%%%%%%%%%%%%%%%%%%%%%%%%%%%%%%%%
for i=1:x
for j=1:n
    di= m2(i)-m(j);
    di=abs(di);
  if ((di<=30)&&(dt(i)==dl(j))&&(mt(i)==ml(j))&&(h2(i)==h(j)))
        fou=TCP(i)/len(j);
        l=len(j);
        lengg=[lengg,l];
        foul=[foul,fou];
        dat=dtcp(i);
        dates=[dates,dat];
  end
  diff=h2(i)-h(j);
  if ((diff==1)&&(di>20)&&(dt(i)==dl(j))&&(mt(i)==ml(j)))
      fou=TCP(i)/len(j);
        l=len(j);
        lengg=[lengg,l];
      foul=[foul,fou];
      dat=dtcp(i);
      dates=[dates,dat];
  end
end
end
foul=foul'
dates=dates'
dtcp=[dt,mt,h2,m2]; dlen=[dl,ml,h,m];
```

**Code 4- Delta TCP between two MCs**

**Description:**

This code calculates the difference in TCP between two MCs using the following equation:

$$\Delta TCP_{MC} = P\left(D_{N+1\,(C)}\right) - P\left(D_{N-1\,(C+1)}\right)$$

Where: $P(D_{N+1\,(C)})$*: TCP during BP for the first BP after MC*

$P(D_{N-1\,(C+1)})$*: TCP during BP for the last BP before next MC*

**Input file:**

Input information should be available in spreadsheet titled, `'UF1_RawData_2017.xlsx'`. The spreadsheet should contain the date and time of each BP, TCP during, after, and before BP, MC type, and RC type. Multiple input files should be used, one for each train and year. Input file layout should be of the same format as input file used for Code 1 (Figure C1)

**Output information:**

This code will output two arrays: `dates` and `ydiff`. The `dates` array contains the date and time of the first of the two MCs. The `ydiff` array contains the change in TCP between the two MCs.

```
clc, clear all, close all
AA=readtable('UF1_RawData_2017.xlsx');
[n,M]=size(AA);

A = xlsread('UF1_RawData_2017.xlsx',1, 'A:A');
B = xlsread('UF1_RawData_2017.xlsx',1, 'B:B');
C = xlsread('UF1_RawData_2017.xlsx',1, 'C:C');
E = xlsread('UF1_RawData_2017.xlsx',1, 'E:E');
F = xlsread('UF1_RawData_2017.xlsx',1, 'F:F');

flag = 0;
index1 = [];index2 = [];first = [];second = [];dates = [];
dates = [dates, AA.Timestamp(1)];
dates1 = [];values = [];values = [B(1), values];

% Fouling intensity due to MC
for i=2:n-1
    if((E(i) == 4 || F(i) == 1|| F(i) == 2) && flag == 0)
        x1 = B(i-1);
        dateTemp = AA.Timestamp(i);
        flag = 1;
    end
    if(flag == 1)
        if(E(i) ~= 4 && F(i) ~= 1 && F(i) ~= 2)
            x2 = B(i);
            index2 = [index2, i];
            flag = 0;
            checkValue = B(i+1) - B(i);

            if(checkValue > 3)
                x2 = B(i+1);
                x1 = B(i);
                dateTemp = AA.Timestamp(i);
            end

            values = [values, x1];
            values = [values, x2];
            dates = [dates, dateTemp];
        end
    end
end
values = [values, B(n)];
[m, N] = size(values);
ydiff = [];
for i=1:2:N-1
    y = values(i) - values(i+1);
    ydiff = [ydiff, y];
end
ydiff'
dates= datetime(dates);
dates'
```

**Code 5- Delta TCP between two RCs**

**Description:**

This code calculates the difference in TCP between two RCs. This is done using the following equation:

$$\Delta TCP_{MC} = P\left(D_{N+1\,(C)}\right) - P\left(D_{N-1\,(C+1)}\right)$$

Where: $P(D_{N+1\,(C)})$*: TCP during BP for the first BP after RC*

$P(D_{N-1\,(C+1)})$*: TCP during BP for the last BP before next RC*

**Input file:**

Input information should be available in spreadsheet titled, `'UF1_RawData_2017.xlsx'`. The spreadsheet should contain the date and time of each BP, TCP during, after, and before BP, MC type, and RC type. Multiple input files should be used, one for each train and year. Input file layout should be of the same format as input file used for Code 1 (Figure C1)

**Output information:**

This code will output two arrays: `datesRC` and `ydiffRC`. The `datesRC` array contains the date and time of the first of the two RCs. The `ydiffRC` array contains the change in TCP between the two RCs.

```
clc, clear all, close all

% Raw Data recalls
AA=readtable('UF1_RawData_2017.xlsx');
[n,m]=size(AA);

B = xlsread('UF1_RawData_2017.xlsx',1, 'B:B');
C = xlsread('UF1_RawData_2017.xlsx',1, 'C:C');
E = xlsread('UF1_RawData_2017.xlsx',1, 'E:E');
F = xlsread('UF1_RawData_2017.xlsx',1, 'F:F');

% Creating empty arrays to store the information
datesRC = [];
valuesRC = [];
flag = 0;

for i=50:n
    % if statement to store the number before code RC (X1)
    if((F(i) == 1) && flag == 0)
        x1RC = B(i-1);
        dateTempRC = AA.Timestamp(i);
        flag = 1;
    end

    % if statement to store the number right after code RC (X2)
    if (flag==1)
        if(F(i) ~= 1)
           x2RC = B(i);
    checkvalue= B(i)- B(i+1);
    if (checkvalue<-2.56)
        x2RC= B(i+1);
        x1RC=B(i);
    end
     flag = 0;
     valuesRC = [valuesRC, x1RC];
     valuesRC = [valuesRC, x2RC];
 datesRC = [datesRC, dateTempRC];
        end
    end
end

[x, y] = size(valuesRC);
ydiffRC = [];
for j=2:2:y-1
 diff = valuesRC(j) - valuesRC(j+1);
  ydiffRC = [ydiffRC, diff];
end

ydiffRC=ydiffRC'
datesRC= datetime(datesRC);
datesRC'
```

**Code 6- Length of Permeation between MC**

**Description:**

This code calculates the length of permeation between two MCs. This is done by counting the number of permeation codes (13XX) between two MCs (58XX).

**Input file:**

Input information should be available in two spreadsheets:

1. Spreadsheet titled, `'MC.xlsx'`: contains the output of Code 4 (See Figure C5)
2. Spreadsheet titled, `'UF1_2017.xlsx'`: contains the date, time, and train status code recorded every minute. Figure C2 displays an example of an input file. Multiple input files should be used, one for each train and year.

| | A | B |
|---|---|---|
| 1 | **Dates** | **Fouling** |
| 2 | 02-Jan-2017 06:49:41 | 17.1692 |
| 3 | 04-Jan-2017 09:20:41 | 14.4921 |
| 4 | 06-Jan-2017 09:36:47 | 17.2463 |
| 5 | 09-Jan-2017 09:24:31 | 4.6995 |
| 6 | 10-Jan-2017 15:45:44 | 3.7524 |
| 7 | 11-Jan-2017 06:20:36 | 12.746 |
| 8 | 13-Jan-2017 09:20:22 | 16.9598 |
| 9 | 16-Jan-2017 09:29:02 | 4.1978 |
| 10 | 17-Jan-2017 03:53:53 | 16.0966 |

**Figure C5- Delta TCP between two MCs (output of Code 4)**

**Output information:**

This code will output one array, `cycle`. The `cycle` array contains the number of minutes of permeation between two MCs.

For fouling slope calculations between two MCs, the output of Code 4 was manually matched to the output of Code 6 (through matching the date of the first of the two MCs). Then Code 4 output was divided by the output of Code 6.

```
clc, clear all, close all

%this code is to determine the length of permeation between two
maintenance
%cleans and recovery cleans

AA=readtable ('MC.xlsx');
[na,ma]=size(AA);
date1=AA.Dates;
d1= datetime(date1,'InputFormat','dd-MM-yyyy HH:mm:ss');
dd1= day(d1);
dm1= month(d1);
[h,m1,s]=hms(d1);
ydiff=AA.Fouling;

BB=readtable('UF1_2017.xlsx');
[nb,mb]=size(BB);
date2= BB.Timestamp;
d2= datetime(date2,'InputFormat','yyyy-mm-dd HH:mm:ss');
dd2= day(d2);
dm2= month(d2);
[h2,m2,s2]=hms(d2);
code= BB.code;

index=[];

for i=1:na
    for j=1:nb
        if
((dm1(i)==dm2(j))&&(dd1(i)==dd2(j))&&(h(i)==h2(j))&&(m1(i)==m2(j)))
           in=j;
           index=[index,in];
        end
    end
end
index=index';
[x,y]=size(index);
count=0;
cycle=[];
for q=1:x-1
    p=index(q);
    p2=index(q+1);
    for z=p:p2
        if ((code(z)==1301)||(code(z)==1302)||(code(z)==1303))
            count=count+1;
        end

    end
    cycle=[cycle,count];
    count=0;
end
cycle=cycle';
```

**Code 7- Length of Permeation between RC**

**Description:**

This code calculates the length of permeation between two RCs. This is done by counting the number of permeation codes (13XX) between two RCs (85XX).

**Input file:**

Input information should be available in two spreadsheets:

1. Spreadsheet titled, `'RC.xlsx'`: contains the output of Code 5 (See Figure C6)
2. Spreadsheet titled, `'UF1_2017.xlsx'`: contains the date, time, and train status code recorded every minute. Figure C2 shows an example of input file. Multiple input files should be used, one for each train and year.

| | A | B |
|---|---|---|
| 1 | **Dates** | **Fouling** |
| 2 | 20-Jan-2016 06:47:26 | 60.2803849 |
| 3 | 13-Feb-2016 14:18:28 | 22.06791385 |
| 4 | 01-Mar-2016 01:49:04 | 26.03996864 |
| 5 | 09-Mar-2016 04:17:45 | 50.77900076 |
| 6 | 16-Mar-2016 02:08:52 | 46.83959738 |
| 7 | 22-Mar-2016 21:39:00 | 46.71648261 |
| 8 | 27-Mar-2016 20:05:34 | 60.2928315 |
| 9 | 02-Apr-2016 18:25:04 | 78.24129658 |
| 10 | 10-Apr-2016 21:57:36 | 81.06661439 |
| 11 | 16-Apr-2016 21:45:56 | 63.85315767 |
| 12 | 23-Apr-2016 22:14:08 | 63.74685041 |

**Figure C6- Delta TCP between two RCs (output of Code 5)**

**Output information:**

This code will output one array, `cycle`. The `cycle` array contains the number of minutes of permeation between two RCs.

For fouling slope calculations between two RCs, the output of Code 5 was manually matched to the output of Code 7 (through matching the date of the first of the two RCs). Then Code 5 output was divided by the output of Code 7.

```
clc, clear all, close all

%this code is to determine the length of permeation between two
maintenance
%cleans and recovery cleans

AA=readtable ('RC.xlsx');
[na,ma]=size(AA);
date1=AA.Dates;
d1= datetime(date1,'InputFormat','dd-MM-yyyy HH:mm:ss');
dd1= day(d1);
dm1= month(d1);
[h,m1,s]=hms(d1);
ydiff=AA.Fouling;

BB=readtable('UF1_2017.xlsx');
[nb,mb]=size(BB);
date2= BB.Timestamp;
d2= datetime(date2,'InputFormat','yyyy-mm-dd HH:mm:ss');
dd2= day(d2);
dm2= month(d2);
[h2,m2,s2]=hms(d2);
code= BB.code;

index=[];

for i=1:na
    for j=1:nb
        if
((dm1(i)==dm2(j))&&(dd1(i)==dd2(j))&&(h(i)==h2(j))&&(m1(i)==m2(j)))
           in=j;
           index=[index,in];
        end
    end
end
index=index';
[x,y]=size(index);
count=0;
cycle=[];
for q=1:x-1
    p=index(q);
    p2=index(q+1);
    for z=p:p2
        if ((code(z)==1301)||(code(z)==1302)||(code(z)==1303))
            count=count+1;
        end

    end
    cycle=[cycle,count];
    count=0;
end
cycle=cycle';
```

**Code 8- Permeability reclamation BP**

**Description:**

This code calculates the reclamation of permeability for BPs using the following equation:

$$R_{BP} = P(A_N) - P(B_N)$$

Where: $P(A_N)$*: TCP after back-pulse*

$P(B_N)$*: TCP before back-pulse*

**Input file:**

Input information should be available in spreadsheet titled, `'UF1_RawData_2017.xlsx'`. The spreadsheet should contain the date and time of each BP, TCP during, after, and before BP, MC type, and RC type. Multiple input files should be used, one for each train and year. Input file should be of the same format as input file used for Code 1 (Figure C1).

**Output information:**

This code will output two arrays: `dates` and `BPreclaim`. The `dates` array contains the date and time of each BP. The `BPreclaim` array contains the change in TCP due to BP.

```
clc, clear all, close all

% Raw Data recalls
AA=readtable('UF1_RawData_2017.xlsx');
[n,m]=size(AA);

B = xlsread('UF1_RawData_2017.xlsx',1, 'B:B');
C = xlsread('UF1_RawData_2017.xlsx',1, 'C:C');
D = xlsread('UF1_RawData_2017.xlsx',1, 'D:D');
E = xlsread('UF1_RawData_2017.xlsx',1, 'E:E');
F = xlsread('UF1_RawData_2017.xlsx',1, 'F:F');

%UF1_RawData_2018.xlsx

BPreclaim=[];
dates=[];

for i=1:(n)
    BP= C(i)-D(i);
    BPreclaim=[BPreclaim, BP];
    d= AA.Timestamp(i);
    dates=[dates, d];
end

BPreclaim'
dates=datetime(dates);
dates'
```

**Code 9- Permeability reclamation MC & RC**

**Description:**

This code calculates the reclamation of permeability for MCs and RCs using the following equation:

$$R_c = P(D_{N+1\,(C)}) - P(D_{N-1\,(C)})$$

Where: $P(D_{N+1\,(C)})$*: TCP during BP for BP immediately after MC or RC*

$P(D_{N-1\,(C)})$*: TCP during BP for BP immediately before MC or RC*

**Input file:**

Input information should be available in spreadsheet titled, `'UF1_RawData_2017.xlsx'`. The spreadsheet should contain the date and time of each BP, TCP during, after, and before BP, MC type, and RC type. Multiple input files should be used, one for each train and year. Input file should be of the same format as input file used for Code 1 (Figure C1).

**Output information:**

This code will output four arrays:

1. `datesMC`: contains the date and time of MC
2. `ReclamationMC`: contains the change in TCP due to MC
3. `datesRC`: contains the date and time of the RC
4. `ReclamationRC`: contains the change in TCP due to RC

```
clc, clear all, close all
AA=readtable('UF1_RawData_2017.xlsx');
[n,m]=size(AA);

B = xlsread('UF1_RawData_2017.xlsx',1, 'B:B');
C = xlsread('UF1_RawData_2017.xlsx',1, 'C:C');
E = xlsread('UF1_RawData_2017.xlsx',1, 'E:E');
F = xlsread('UF1_RawData_2017.xlsx',1, 'F:F');
flag = 0;

ReclamationMC = [];
index1 = [];index2 = [];first = [];second = [];
dateMC = [];

%for the RCs
ReclamationRC= [];index1RC = [];index2RC = [];
firstRC = [];
secondRC = [];
dateRC = [];

% Reclamation due to MC
for i=1:n-3
    if(E(i) == 4 && flag == 0)
        x1 = B(i-1);
        index1 = [index1, i-1];
        first = [first, x1];
        flag = 1;
        dateMC = [dateMC, AA.Timestamp(i)];
    end
    if(flag == 1)
        if(E(i) ~= 4)
            x2 = B(i);
            index2 = [index2, i];
            second = [second, x2];
            flag = 0;
            y = x2-x1;
            checkValue = B(i+1) - B(i);
             if (checkValue> y)
                x2 = B(i+1);
                x1= B(i);
                y = x2-x1;
             end

            if(checkValue > 8)
                x2 = B(i+1);
                x1= B(i);
                y = x2-x1;
            end

            if(y < 0)
                x1 = B(i);
                x2 = B(i+1);
                y = x2-x1;
            end
```

```
            ReclamationMC = [ReclamationMC, y];
        end
    end
end

dateMC = datetime(dateMC);
ReclamationMC= ReclamationMC';
dateMC= dateMC';

ReclamationMC;
dateMC

% Reclamation due to RC
for i=1:n-3
    if((F(i) == 1 ||F(i) == 2) && flag == 0)
        x1RC = B(i-1);
        index1RC = [index1RC, i-1];
        firstRC = [firstRC, x1RC];
        flag = 1;
        dateRC = [dateRC, AA.Timestamp(i)];
    end
    if(flag == 1)
        if(F(i) ~= 1)&&(F(i)~= 2)
            x2RC = B(i);
            index2RC = [index2RC, i];
            secondRC = [secondRC, x2RC];
            flag = 0;
            yRC = x2RC-x1RC;
            checkValue = B(i+1) - B(i);

            if(checkValue > 8)
                x2RC = B(i+1);
                x1RC= B(i);
                yRC = x2RC-x1RC;
            end

            if(y < 0)
                x1RC = B(i);
                x2RC = B(i+1);
                yRC = x2RC-x1RC;
            end
            ReclamationRC = [ReclamationRC, yRC];
        end
    end
end

%Results for RC
dateRC = datetime(dateRC);
ReclamationRC=ReclamationRC';
dateRC= dateRC'
```

**Code 10- Permeate temperature of each cycle**

**Description:**

This code estimates the permeate temperature during a specific cycle based on the temperature data available on InSight, that were recorded every 15 minutes.

**Input file:**

Input information should be available in spreadsheet titled, `'TempMatch.xlsx'`. The spreadsheet should contain the date and fouling indexes calculated for each cycle using Code 3 (Columns A & B). The spreadsheet should also contain the temperature data recorded every 15 minutes (Columns C & D). Figure C7 displays an example of the layout of input file.

| | A | B | C | D |
|---|---|---|---|---|
| 1 | **Date1** | **Fouling Index** | **Date2** | **Temp** |
| 2 | 2018-01-01 6:35 | 0.336614 | 01/01/2018 00:00:00 | 11.76201 |
| 3 | 01-Jan-2018 10:53:56 | NaN | 01/01/2018 00:15:00 | 11.76428 |
| 4 | 01-Jan-2018 16:30:27 | 0.186134783 | 01/01/2018 00:30:00 | 11.80172 |
| 5 | 01-Jan-2018 21:35:45 | 0.383346875 | 01/01/2018 00:45:00 | 11.7484 |
| 6 | 02-Jan-2018 04:46:03 | 0.243558333 | 01/01/2018 01:00:00 | 11.73479 |
| 7 | 02-Jan-2018 10:23:57 | 0.214766154 | 01/01/2018 01:15:00 | 11.72684 |
| 8 | 02-Jan-2018 13:13:23 | 0.463446753 | 01/01/2018 01:30:00 | 11.72798 |
| 9 | 02-Jan-2018 19:30:02 | NaN | 01/01/2018 01:45:00 | 11.80286 |
| 10 | 03-Jan-2018 14:57:26 | 0.334307339 | 01/01/2018 02:00:00 | 11.79265 |
| 11 | 03-Jan-2018 19:04:53 | 0.370919231 | 01/01/2018 02:15:00 | 11.66898 |

**C7- Layout of input file**

**Output information:**

This code will output two arrays: `dateTemp` and `temp`. The `dateTemp` array contains the date and time of each cycle. The `temp` array contains the temperature of the permeate estimated for a specific cycle.

```
clc, clear all, close all, format long

%this code will be finding the exact temperature during each of the
backwashes
AA=readtable ('TempMatch.xlsx');
[n,m]= size(AA);
date=AA.Date1;
d1= datetime(date,'InputFormat','dd-MMM-yyyy HH:mm:ss');
% date 1 is the data for the backwash (i)
dd1= day(d1);
dm1= month(d1);
[h,m1,s]=hms(d1);

date2=AA.Date2;
d2= datetime(date2,'InputFormat','MM/dd/yyyy HH:mm:ss');
% date 2 is the data for the temperature (j)
dd2= day(d2);
dm2= month(d2);
[h2,m2,s2]=hms(d2);

temp=[]; dateTemp=[];
%%%%%%%%%%%%%%%%%%%%%%%%%%%%%%%%%%%%%%%%%%%%%%%%%%%%%%%%
for i=1:1860
    for j=1:n-1
        diffm= abs(m1(i)-m2(j));
        diffm2= abs(m1(i)-m2(j+1));
        diffh= (h(i)- h2(j+1));
        diffd=dd1(i)-dd2(j+1);
       if (diffm<=7)&&((dd1(i)==dd2(j))&&(dm1(i)==dm2(j))&&(h(i)==h2(j)))
         t=AA.Temp(j);
         temp=[temp,t];
         dd=d1(i);
         dateTemp=[dateTemp,dd];
       end
        if (diffm>7)&&((dd1(i)==dd2(j))&&(dm1(i)==dm2(j))&&(diffh==-
1))&&...
                (diffm2>=53)
         t=AA.Temp(j+1);
         temp=[temp,t];
         dd=d1(i);
         dateTemp=[dateTemp,dd];
        end
        if (diffm>7)&&(diffd==-1)&&(dm1(i)==dm2(j))&&(diffh==23)&&...
           (diffm2>=53)
         t=AA.Temp(j+1);
         temp=[temp,t];
         dd=d1(i);
         dateTemp=[dateTemp,dd];
       end
    end
end

temp=temp';
dateTemp=dateTemp'
```